CHAPTER 6 US-Japan Joint Research Projects Overview

The US-Japan Joint Research Projects have decades of rich and successful history contributing to advancing fusion materials science and enabling technologies, with FRONTIER as the latest, ongoing project. These projects are defined and approved by the Coordinating Committee on Fusion Energy (CCFE) under the "Agreement between the Government of the United States of America and the Government of Japan on Cooperation in Research and Development in Energy and Related Fields" signed in 1979. Since the first project, RTNS-II that started in 1981, the core research subjects have evolved from fundamental radiation materials science focusing on the effects of fusion spectrum neutrons to increasingly include applied science and enabling technologies for magnetic confinement fusion energy (Table 1); however, the effects of neutron irradiation in fusion materials and components has remained the undeviating technical backbone. The use of unique US experimental capabilities and key facilities has been among the principles of collaboration.

Table 1. History of the US-Japan Joint Research Projects on fusion materials and technologies.

Project Title	Period*	Key Facility	Core Subject
RTNS-II	1981–1986	RTNS-II	Low-dose D-T neutron irradiation
FFTF/ MOTA	1987–1994	FFTF, EBR-II	High-fluence neutron irradiation
JUPITER	1995–2000	HFIR, ATR, HFBR	Non-steady and transient radiation effects
JUPITER -II	2001–2006	HFIR, STAR, MTOR	Key issues for advanced blanket concepts
TITAN	2007–2012	HFIR, TPE, MTOR, PISCES	Thermofluid, n-T synergism, coating, and joining
PHENIX	2013–2018	HFIR, PAL, TPE	Tungsten-based, helium-cooled PFC technologies
FRONTIER	2019–2024	HFIR, TPE	Interface elements in PFC

*Japanese fiscal year.

6.1 Objectives, Research Subjects, and Facilities

During the last decade, the US-Japan Joint Research Projects evolved the TITAN (Tritium, Irradiation and Thermofluid for America and Nippon) that concluded in JFY-2012,

PHENIX (Technological Assessment of Plasma Facing Components for DEMO Reactors) that started in JFY-2013 and concluded in JFY-2018, and FRONTIER (Fusion Research Oriented to Neutron Irradiation Effects and Tritium Behavior at Material Interfaces) that is currently in its early phase after starting in JFY-2019. Each of these projects had/has a performance period of six years.

Highlights from the technical accomplishments in each task and the irradiation program are given in the following subsections.

TITAN – The TITAN project focused on advancing scientific understanding of the effects of complex operating environments of fusion reactors on the behaviors of hydrogen isotopes and (magneto-) thermofluid dynamics in the blanket, first wall, and fuel recovery systems. The TITAN project contributors were from NIFS, INL, ORNL, and a number of universities including UCLA and UCSD in USA and nine different universities in Japan. The project was unique in integrating these fusion fuel cycle and liquid metal and salt blanket technology issues with the effects of neutron irradiation on properties and interfacial behaviors of the blanket and first wall materials [1]. This was a pioneering effort of an integrated multi-scale, multi-physics approach in understanding the performance of material systems in environments that couple extreme operating conditions. It pioneered today's trend in performance modeling of nuclear energy systems. A dedicated overview of the TITAN project is given later in this Section.

PHENIX – The acronym PHENIX stands for PFC Evaluation by Tritium Plasma, Heat and Neutron Irradiation Experiments. The main project goal was to evaluate the technical feasibility of helium-cooled, tungsten-armored divertor concepts, which include several high technical risks, high pay-off options for fusion DEMO divertors with outstanding safety characteristics [2]. Understanding the effects of neutrons, heat loading, and plasma exposure is the overarching goal of PFC materials science. Among the various technical issues for PFCs, the PHENIX project examined the heat transfer and high-heat-load responses, effects of neutron irradiation, and the hydrogen isotope behaviors.

The PHENIX project consisted of three technical tasks: Task 1, Heat Flow Response; Task 2, Neutron Effects in Materials; and Task 3, Tritium Behavior. As depicted in Fig. 1, Task 1 dealt with issues related to heat load and flux, including the high heat load in armor materials, heat transfer from the armor through a structural cartridge to the helium coolant, and the high-pressure/high-temperature helium flow in the multi-jet impingement cooling. The main experimental facilities for Task 1 were the High Heat Flux Test Station at the Plasma Arc

Lamp (PAL) facility at ORNL and the helium loop facility at the Georgia Institute of Technology.

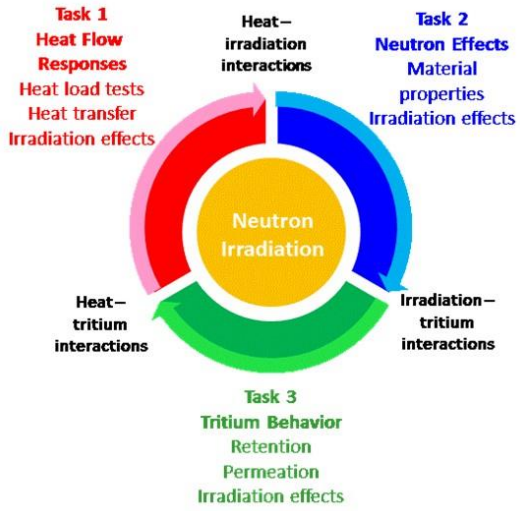

Fig. 1. Task structure and inter-relations in PHENIX project.

Task 2 on Neutron Effects determined the effects of neutron irradiation at PFC-relevant temperatures on the thermal, mechanical, and physical properties of tungsten materials, in response to the critical demands for reliable data for properties of neutron-irradiated tungsten. The outcome from this task enabled greatly improved fidelity of modeling and integrity assessment for PFC structures. This task mainly used the 3025E hot cell facility, the Low Activation Materials Development and Analysis (LAMDA) Laboratory, and the associated microscopy center at ORNL (Fig. 2).

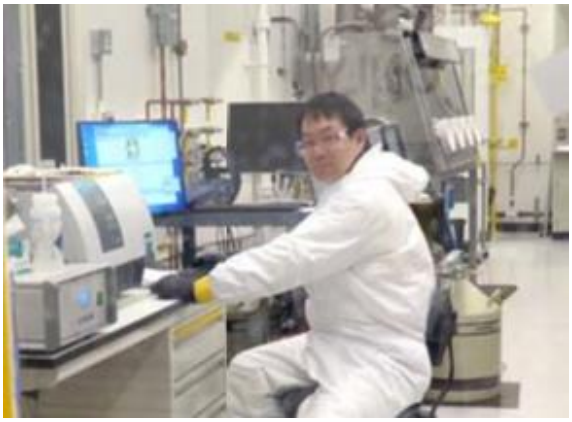

Fig. 2. Visiting researcher from Osaka Prefectural University, Japan, conducting post-irradiation examination at Oak Ridge National Laboratory.

Task 3 on Tritium Behavior focused on the retention and permeation of hydrogen isotopes in neutron-irradiated tungsten. The Tritium Plasma Experiment (TPE) facility located at Idaho National Laboratory (INL) served as the primary experimental capability (Fig. 3). In addition, various additional facilities in US and Japan were used for measurements of deuterium permeation, thermal desorption, and depth profiling.

Fig. 3. Visiting researcher from Hokkaido University, Japan, participating an experiment at Idaho National Laboratory with US research scientist.

Neutron irradiation program served as a core function of the PHENIX project as it provided all three technical tasks with a consistent and systematic set of irradiated test specimens. The planning for the irradiation program, test matrix development, capsule development and construction, and execution of irradiation were conducted in collaboration with all tasks.

FRONTIER – with the successful conclusion of the PHENIX project, a great deal of critical knowledge was developed in areas of heat flow and removal, baseline properties and hydrogen isotope interactions of tungsten materials, and the effects of neutron irradiation on all of these. The FRONTIER project, building upon and complementing the preceding project, will address the scientific questions related to the neutron and hydrogen isotope interactions with the interfacial and transition elements in advanced PFCs. Such elements include the solid-solid interfaces within the plasma-facing materials and components, the solid-solid transitions in advanced PFCs, the solid-liquid interfaces in the liquid metal PFC systems, and the PFC-oxidant-tritium interactions in liquid cooled and liquid surface concepts. Interface effects in the materials integration enabled by advanced manufacturing and accident events are included. The FRONTIER research addresses the evolving research needs arising from the rapid PFC innovations.

6.2 Administration and Operations Management

In coordinating these six-year projects with funding uncertainties and evolving availability/functionality of the key resources, the annual Steering Committee Meetings (SCMs) played a critical role (Fig. 4). In each project, a total of seven SCMs were held with participation by the Representative, Program Coordinator, Task Coordinators and additional key people from both the US and Japan. The administration structures of PHENIX and FRONTIER projects are given in Tables 2 and 3. The TITAN project administration is found in the next subsection. In addition to the SCMs, topical workshops were organized typically a few times a year across multiple tasks. These workshops served as the venue to discuss; detailed technical planning, integration of technical tasks and irradiation plans, discussion of the experimental results, and exchange of other relevant information.

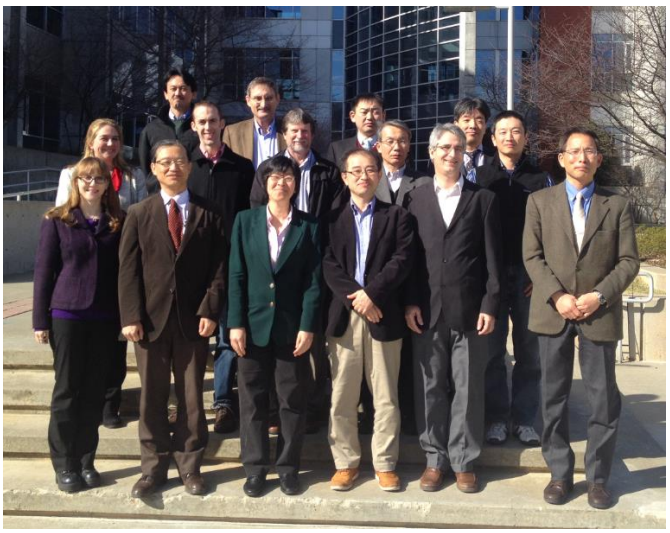

Fig. 4. Photo from the 3rd PHENIX Steering Committee Meeting, held in 2015 at Georgia Institute of Technology.

Table 2. Administrative structure of PHENIX project.

Steering Committee

	Japan	USA
Representative	Y. Ueda (Osaka U.)	P. Pappano / D. Clark (DOE)
Program Coordinator	Y. Hatano (U. Toyama)	P. Pappano / D. Clark (DOE)

Task Coordinators and Deputies

	Japan	USA
Task 1 Heat Flow Responses	T. Yokomine (Kyoto U.) Y. Ueda (Osaka U.)	M. Yoda (GA Tech) A. Sabau (ORNL)
Task 2 Neutron Effects	T. Hinoki (Kyoto U.) A. Hasegawa (Tohoku U.)	Y. Katoh / L. Garrison / J.W. Geringer (ORNL)
Task 3 Tritium Behavior	Y. Oya (Shizuoka U.) Y. Hatano (U. Toyama)	B. Merrill / M. Shimada (INL) D. Buchenauer (SNL)

Table 3. Administrative structure of FRONTIER project.

Steering Committee

	Japan	USA
Representative	Y. Hatano (U. Toyama)	D. Clark (DOE)
Program Coordinator	T. Yokomine (Kyoto U.)	Y. Katoh (ORNL)

Task Coordinators and Deputies

	Japan	USA
Task 1 Solid-Solid Interfaces	T. Hinoki (Kyoto U.) N. Hashimoto (Hokkaido U.)	L. Garrison / X. Hu / W. Geringer (ORNL)
Task 2 Tritium Transport Accident Safety	Y. Oya (Shizuoka U.) T. Otsuka (Kindai U.)	M. Shimada (INL) R. Kolasinski (SNL)
Task 3 Solid-Liquid Interfaces	M. Kondo (TITECH) J. Miyazawa (NIFS)	B. Pint / J. Jun (ORNL)
Task 4 Divertor Systems Analysis	T. Yokomine (Kyoto U.)	C. Kessel (ORNL)

References

[1] T. Muroga, D.K. Sze, K. Okuno, T. Terai, A. Kimura, R.J. Kurtz, A. Sagara, R. Nygren, Y. Ueda, R.P. Doerner, B.J. Merrill, T. Kunugi, S. Smolentsev, Y. Hatano, T. Yamamoto, A. Hasegawa, Y. Katoh, Research on Tritium/Heat Transfer and Irradiation Synergism for First Wall and Blanket

in the TITAN Project, in: 24th IAEA Fusion Energy Conf., International Atomic Energy Agency, San Diego, 2012.

[2] Y. Katoh, D. Clark, Y. Ueda, Y. Hatano, M. Yoda, A.S. Sabau, T. Yokomine, L.M. Garrison, J.W. Geringer, A. Hasegawa, T. Hinoki, M. Shimada, D. Buchenauer, Y. Oya, T. Muroga, Progress in the U.S./Japan PHENIX project for the technological assessment of plasma facing components for DEMO reactors, Fusion Sci. Technol. 72 (2017) 222–232. doi:10.1080/15361055.2017.1333868

TITAN Overview

Category: TITAN/PHENIX/FRONTIER
Name: T. Muroga
Affiliation: NIFS

1. Introduction

The joint projects by Japan (NIFS and Universities) and USA under the Fusion Cooperation Program have a history of almost 40 years. The TITAN project (Tritium, Irradiation and Thermofluid for America and Nippon) was carried out through six years (FY 2007-2012). Before TITAN, four joint projects have been carried out. The initial three projects (RTNS-II, FFTF/MOTA, and JUPITER) focused on neutron irradiation effects on fusion materials using neutron irradiation and post irradiation examination (PIE) facilities in the US. The next project (JUPITER-II) extended the subject of the initial projects to include key issues for advanced blankets using facilities for tritium and thermofluid tests in the US, in addition to those for neutron irradiation [1].

The use of unique US facilities is the major incentive in this collaboration. The contributions of the Japanese side include the supply of high-quality test materials and characterization technologies for microstructures, mechanical properties, tritium distribution, thermofluid performance, and others.

2. Objective and task structure

The TITAN project has a broader scope than the JUPITER-II project by including first wall issues and interface issues among the first wall, blanket, and recovery system. Particular emphasis was placed on obtaining fundamental understanding for establishing tritium and thermofluid control. The experiments were designed for testing under conditions specific to fusion, such as intense irradiation, high heat/particle flux, and circulation in a high magnetic field. The results were applied using integrated modeling to advance the design of tritium and heat control in MFE and IFE systems.

Table 1 summarizes the tasks, subtasks, facilities, and research subjects. The project has three tasks and seven subtasks. Task 1 is about transport phenomena that consider mass and heat flow in the first wall, blanket, and recovery system. Special emphasis is placed on mass transfer during the interaction of mixed plasma of D/He/Be with the first wall, tritium transfer in liquid breeders, and the thermofluid control in liquid breeders in a magnetic field. Task 2 focuses on the irradiation effects of materials with an emphasis on the synergistic effects of irradiation and tritium or other impurities including transmutation-induced helium. The common task is a unique group organized by those who are engaged in other tasks and take care of the modeling. This task performs integration modeling of materials performance, thermofluids in

Table 1. Organization of the TITAN project as of April 2011

Representatives Coordinators		JP : K. Okuno (Sizuoka U.) JP : T. Muroga (NIFS)		US : G. Nardella (USDOE) US : D. Sze (UCSD)		
Task	Subtask	Facility	TC (JP)	STC/Deputy (JP)	TC (US)	STC/Deputy (US)
Task 1 Transport phenomena	1-1 Tritium and mass transfer in first wall (concluded March 2010)	TPE PISCES	T. Terai (U.Tokyo)	Y. Ueda (Osaka U.)/ N. Ohno (Nagoya U.) K. Tokunaga (Kyushu U.)	D. Sze (UCSD)	R. Doerner (UCSD)
	1-2 Tritium behavior in blanket systems	STAR		T. Terai (U. Tokyo)/ S. Fukada (Kyushu U.) S. Konishi (Kyoto U.)		P. Calderoni(INL)
	1-3 Flow control and thermofluid modeling	MTOR		T. Kunugi (Kyoto U.)/ T. Yokomine (Kyoto U.)		S. Smolentsev (UCLA)/ K. Messadek (UCLA)
Task 2 Irradiation synergism	2-1 Irradiation-tritium synergism	HFIR STAR	A.Kimura (Kyoto U.)	Y. Hatano (Toyama U.)/ Y. Oya (Shizuoka U.)	R. Kurtz (PNNL)	M. Sokolov (ORNL)/ Y. Katoh (ORNL) P. Calderoni (INL)
	2-2 Joining and coating integrity	HFIR ORNL-HL (incl. T-test)		A. Kimura (Kyoto U.)/ N. Hashimoto (Hokkaido U.) T. Nagasaka (NIFS)		T. Yamamoto (UCSB)/ M. Sokolov (ORNL)
	2-3 Dynamic deformation			A.Hasegawa (Tohoku U.)/ T. Hinoki (kyoto U.)		Y. Katoh (ORNL)
Common Task System integration modeling	MFE/IFE system integration modeling		A.Sagara (NIFS)	A. Sagara (NIFS)/ H. Hashizume (Tohoku U) T. Norimatsu (Osaka U.)	R. Nygren (SNL)	R. Nygren (SNL)
Laboratory Liaisons	ORNL : R. Stoller (ORNL) INL : B. Merrill (INL) IMR-Oarai (Tohoku) : T. Shikama (Tohoku U.)					
IFE Liaisons		K. Tanaka (Osaka U.)		Kodama(Osaka U.) Yoneda(UTC)	M. Tillack (UCSD)	

magnetic fields, tritium and mass transfer for the enhancement of reactor system design, including the evaluation of the available modeling codes and the enhancement of reactor system designs

3. Facilities used

The following US facilities are used.

(a) STAR (Safety and Tritium Applied Research) [INL] Established at the Idaho National Laboratory in 2001, with an allowable tritium inventory of 16,000 Ci, STAR includes the Tritium Plasma Experiment (TPE) and various facilities for testing tritium behavior in blanket conditions. Unique features of the facility include use of Be and neutron-irradiated materials.

(b) HFIR (High Flux Isotope Reactor) [ORNL] HFIR is a 100MW mixed spectrum research reactor, currently operated at 85MW, which is planned to remain in operation until 2035. The HFIR is a unique irradiation facility with the potential for high environmental and temperature control during irradiation, and very low to high flux irradiation. Some of the HFIR-irradiated specimens were shipped to Oarai Center of Tohoku University for PIE.

(c) MTOR (Magneto-Thermofluid Omnibus Research Facility) [UCLA] The facility includes a magnet of homogeneous field to 2T in an area 15cm wide and 1m long, which can be used for testing the fluid dynamics of liquid metals and MHD flow for high Prandtl number simulant fluids using electrolytes.

(d) PISCES (Plasma Interactive Surface Component Experimental Station) [UCSD] A linear plasma simulator which can produce high-density plasmas with H, D, He and Be. Pulsed lasers are equipped for synergistic plasma exposure and pulse heating studies. Plasma diagnostics and surface characterization systems are furnished.

A quite unique effort initiated in the TITAN project is to send radioactive samples from ORNL to INL allowing tritium tests and plasma exposure for neutron irradiate materials. This activity is continuing throughout TITAN, PHENIX and FRONTIER projects.

4. Project progress

The TITAN project started in April 2007. The budget available for the project (~1.0 M$ from each side) was almost steady in the first three years with a minor decline. However, sizable budget reduction occurred in FY2010 (down to ~0.74 M$ each). Re-planning of the project, including downsizing of test matrices and tasks restructuring, was made to accommodate the budget cuts. Task 1-1 was decided to be concluded as of March 2010. The TPE part of the task was merged to Task 2-1, and some of the research projects in PISCES continued outside the TITAN budget by Japanese scientists assigned to UCSD.

5. Summary of the achievements

The research highlights were published in refs. [2,3]. They are outlined as follows.

(1) Tritium diffusion into bulk for PFM was evaluated using T plasma. Effects of mixed plasma by He/Be/D was elucidated.

(2) Basic data for tritium solubility in Li-Pb and tritium permeation barrier performance were obtained.

(3) It was demonstrated that MHD pressure drop of Li-Pb can be mitigated by three-sided insulation wall.

(4) Irradiation effects on deuterium inventory and diffusion was evaluated by D plasma exposure of neutron-irradiated samples.

(5) Neutron irradiation effects on advanced coating and joining for blanket application were investigated.

(6) Radiation creep of ceramics materials was evaluated using a newly developed method.

(7) System integration modeling was carried out to enhance the contribution of the present results to reactor and blanket design.

References

[1] K. Abe, A. Kohyama, S. Tanaka, C. Namba, T. Terai, T. Kunugi, T. Muroga, A. Hasegawa, A. Sagara, S. Berk, S.J. Zinkle, D.K. Sze, D.A. Petti, M.A. Abdou, N.B. Morley, R.J. Kurtz, L.L. Snead, N.M. Ghoniem, Fusion Engineering and Design, 83 (2008) 842-849.

[2] T. Muroga, D.K. Sze, K. Okuno et al., Fusion Science and Technology, 60 (2011) 321-328.

[3] T. Muroga, D.K. Sze, K. Okuno, Fusion Engineering and Design, 87 (2012) 61

Task 1: Heat Transfer Tests

Category: PHENIX
Name: M. Yoda, S.I. Abdel-Khalik / T. Yokomine
Affiliation: Georgia Tech / Kyoto University

(a) Task 1a: Understanding Heat Transfer and Fluid Flow

The objective of this task was to perform experimental studies of a tungsten-alloy test section modeling the helium-cooled divertor with multiple-jet cooling (HEMJ). A helium (He) test loop pressurized to 10 MPa was built at Georgia Tech (GT) with a maximum He mass flow rate $\dot{m}$ = 10 g/s and a maximum He inlet temperature T_i of 350 °C.

A HEMJ test section consisting of a WL10 outer shell and AISI 304 stainless inner shell (Fig. 1 inset) was fabricated based on the J1c design, heated by a 10 kW radio-frequency induction heater from the Idaho National Laboratory via a water-cooled copper coil. The data, obtained at incident heat fluxes as great as 8 MW/m^2 (based on an energy balance on the He)[1] agree with our earlier correlation for the dimensionless heat transfer coefficient (HTC) or Nusselt number $\overline{Nu} = 0.045\, Re^{0.67}\, \kappa^{0.19}$ (Fig. 1)[2] where the Reynolds number Re is the dimensionless $\dot{m}$ and κ is the ratio of the thermal conductivities of the WL10 and He. The dimensionless pressure drop across the HEMJ test section K_L ≈ 3.2 for $T_i \geq 300$ °C, and is essentially independent of Re.

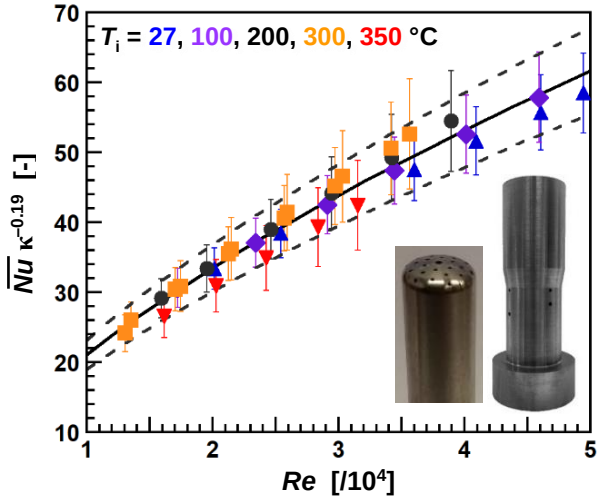

Fig. 1. Experimental data (points) and correlation (solid line; dashed lines ±10% error bounds) for Nusselt number $\overline{Nu}$ as a function of Reynolds number and thermal conductivity ratio κ. The insets show the inner jets cartridge and outer shell.

The $\overline{Nu}$ correlations and K_L results were extrapolated to prototypical conditions to estimate the thermal performance of the HEMJ. These extrapolations suggest that the hexagonal tile (*i.e.*, plasma-facing surface) of the HEMJ can, for a maximum pressure boundary temperature of 1200 °C, accommodate maximum steady-state heat fluxes of 11.5 MW/m^2 and 9.9 MW/m^2 at T_i = 600 °C and 700 °C, respectively, at a pumping power fraction β of the total incident thermal power of 10% and 18%, respectively.

(b) Task 1b: Optimization of Cooling Configuration

The objective of this task was to simplify the complex geometry of the HEMJ, which involves 25 jets issuing from holes of two different diameters issuing from and impinging on a curved surface (Fig. 1 inset), without compromising thermal performance. Coupled computational fluid dynamics and thermal stress simulations were used to model various configurations of fewer jets issuing from holes of the same diameter on a flat surface. The total cross-sectional area of the jets was constrained to be the same as that for the HEMJ.

The simulations suggested that the most promising candidate, the "flat design," with seven jets issuing from 1.18 mm diameter holes on a flat surface (Fig. 2 inset), had a somewhat higher average HTC and slightly lower maximum von Mises stress on the cooled (WL10) surface.[3] Very recent experimental studies of this configuration in the GT He loop suggest that this design has $\overline{Nu}$ that are about 10% higher than those predicted by the HEMJ correlation at the prototypical $Re = 2.1\times10^4$ (Fig. 3). These results suggest that simpler finger-type modular divertor designs that can withstand ITER-like steady-state heat fluxes are feasible with suitable development.

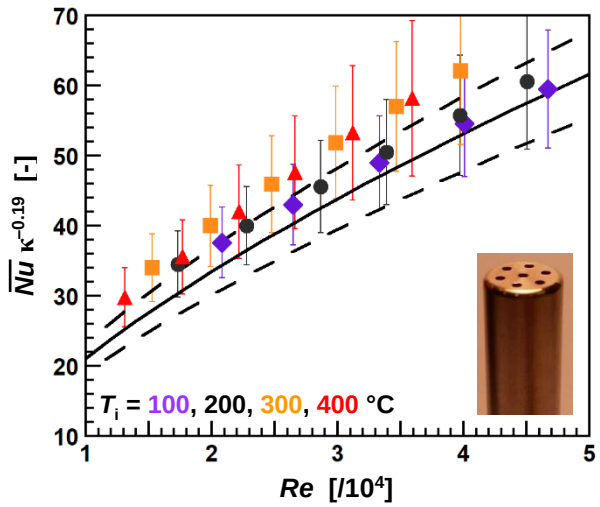

Fig. 2. Experimental data (points) for the flat design compared with the correlation (solid line; dashed lines ±10% error bounds) for the HEMJ for $\overline{Nu}(Re, \kappa)$. The inset shows the inner jets cartridge of the flat design.

1) D. S. Lee *et al.*, Fusion Sci. & Tech., 75 (2019) 873
2) B. H. Mills *et al.*, Fusion Sci. & Tech., 68 (2015), 541
3) B. Zhao *et al.*, Fusion Eng. & Des., 136 (2018), 67

High Heat Flux Testing of Plasma-Facing Materials for Fusion

Category: PHENIX
Name: A. Sabau/L. Garrison/K. Tokunaga/K. Ibano
Affiliation: ORNL/Kyushu University/Osaka University

Task 1 of the six-year US-Japan PHENIX collaboration included high-heat flux (HFF) testing of neutron-irradiated W materials. The objective of the HHF effort was to determine how changes in material properties due to neutron irradiation will affect the performance of plasma-facing components, especially tungsten (W). The HHF plasma-arc lamp (PAL) facility at ORNL was used for this study. The experiments were complemented by finite-element simulation of thermal loads and stresses.

Assessing the effect of neutron irradiation on plasma-facing materials is difficult due both to technical and radiological challenges. In an effort to address the radiological challenges, a new HHF facility based on water-wall plasma-arc lamps was developed at ORNL [1] and upgraded recently [2]. *The first accomplishment* was the successful demonstration of safe HHF testing of low radioactivity level irradiated materials using unbolted W neutron-irradiated specimens at 1.6 MW/m^2 absorbed heat flux (incident 3.5 MW/m^2) in a low-vacuum controlled atmosphere [3]. *The second accomplishment* was the design of specimen holders to bolt the so-called "small-and-thin material specimens" (STMS) specimen onto actively cooled Cu modules. Six vacuum plasma-sprayed (VPS) W-on-F82H low activation steel [4] STMS were successfully HHF tested at 1.6 MW/m^2 on the bolted mounting [5, 6]. *The third accomplishment* was the development of a simplified 3D thermo-mechanical Finite Element Analysis (FEA) model that was used to understand the complex deformation of the bimetallic F82H/W specimens during HHF [5, 6]. Numerical simulation results for one HHF cycle, which were obtained with a FEA model that considers the specimen bolting effect in the VPS-W and F82H, were found to qualitatively reproduce the experimentally observed deformation of the specimen [5]. The predicted stress levels using the FEA model during one HHF cycle in the VPS-W, were found to exceed the failure stress of the brittle VPS-W layer near the clamped edges of the specimen and this explains the observed cracking of a W/F82H specimen during HHF. *The fourth accomplishment* was the design, fabrication, and testing of a new PAL reflector to attain fusion-prototypical steady-state absorbed heat fluxes in W of 6 MW/m^2 (incident 12 MW/m^2) over a 2 cm wide strip [2]. The new reflector was designed with side ports to allow the external mounting of a pyrometer with direct line-of-sight to the specimen, enabling the direct measurement the specimen temperature using pyrometers. *The fifth accomplishment* was the upgrade of the bolting specimen holder to withstand 6 MW/m^2 (incident 12 MW/m^2) heat fluxes provided by the new reflector while enabling (a) the highest thermal gradient through the specimen and (b) the use of thermocouples underneath the sample to measure back-side temperatures (Figure 1a) [2].

To simulate on/off cycling of normal operating plasma, target temperatures of 950 to 1,150°C were sought for the top surface of the specimen while actively cooling the specimen on its back surface to attain a high thermal gradient. Target sample surface temperatures were obtained by employing 4.7/5.1 MW/m^2 (incident 11.0/11.9 MW/m^2) HHF cycles of 2–3 s duration with 60–80 s cooling time between cycles. The measured temperature data indicate that the target surface temperature was attained (Figure 1b). Moreover, surface examination indicated that the back surface of the specimen was in good thermal contact with the actively cooled Cu during HHFT.

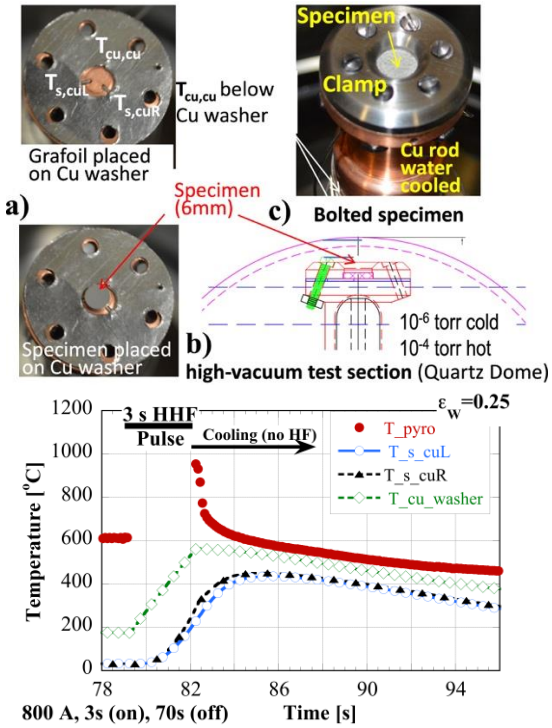

Figure 1. (a) Thermocouple placement, specimen mounting, and confined test section, and (b) Measured temperatures for a 3s heat flux pulse of 4.7 MW/m^2. The PAL was immediately shutdown after the HHF pulse.

The sixth accomplishment was the successful HHF exposure of 7 W-based samples, including two neutron-irradiated samples [7]. The tested materials were thick plate "ITER type" W produced by ALMT and K-doped W-3%Re. Both materials had samples prepared in two orientations: with the grains elongated perpendicular to or parallel to the sample surface. These 6 mm diameter and 2 mm thick samples were irradiated in the HFIR RB*19J capsule that used thermal neutron shielding to better approximate the transmutation rates of a fusion reactor.

To simulate on/off cycling of a normal operating plasma, samples were exposed to approximately 800-900 cycles at 4.7 MW/m^2 absorbed heat flux (incident heat fluxes of 11.0 MW/m^2) [7]. After PAL exposure, scanning electron microscopy examination showed slight changes on the surfaces of the pure W samples. The samples showed some annealing in the near surface polished region, but all eignt samples tested were below the damage threshold for cracking or other destructive changes [7]. While these HHF conditions do not exactly replicate the conditions of a particular fusion reactor, they serve as baseline experimental data for future modeling and simulation. The ultimate goal is the modeling-based design of plasma-facing components.

[1] A.S. Sabau, E.K. Ohriner, J.O. Kiggans, et al., Phys. Scripta T159, 014007 (2014)

[2] Sabau, A. S., Tokunaga, K., Littleton, M. et al., Fusion Sci. Tech 75 no 7 (2019): 690-701.

[3] A.S. Sabau, E.K. Ohriner, J.O. Kiggans, et al., Fusion Sci. Tech 66, 394 (2014)

[4] K. Tokunaga, T. Hotta, K. Araki, et al., J. Nucl. Mat 438, S905 (2013)

[5] Ibano, K., A. S. Sabau, K. Tokunaga, et al., *Nucl. Mater. and Energy* 16 (2018): 128-132.

[6] A.S. Sabau, K. Tokunaga, S. Gorti, et al., To be submitted to Fusion Sci. Tech. (April 2021).

[7] Garrison, L. M., Sabau, A. S., Gregory, B., et al. *Phys. Scripta* T171, 014077 (2020).

Task 1: Investigation of Overall Heat Flow Response in Plasma-Facing Components

Category: PHENIX
Name: T. Yokomine[1], Y. Ueda[2], K. Yuki[3], K. Tokunaga[4], M. Akiyoshi[5], K. Ibano[2], M. Yoda[6], A. Sabau[7]
Affiliation: [1]Kyoto Univ., [2]Osaka Univ., [3]Sanyo-Onoda City Univ., [4]Kyushu Univ., [5]Osaka Pref. Univ., [6]GIT, [7]ORNL

Plasma Facing Components (PFC) are subject to steady/unsteady heat load and particle load at the same time. As a result, the effects of thermal stress, thermal fatigue, hydrogen / He, etc. are additive on the plasma facing material, and there is concern that the integrity of the PFC may deteriorate due to damage or embrittlement of the materials. The flow of heat and particles is regarded as a primary safety phenomenon in PFC where robust design is required. Ideally, the overall heat flow in PFC should be simulated experimentally, but in addition to the difficulty of reproducing nuclear heat generation, it is almost impossible to carry out simultaneous material and cooling performance tests for safety analysis. Therefore, in this task, the material heat load test and heat transfer experiment on the plasma facing material under high heat flux are performed separately. By combining the results, we aimed to provide safety evaluation criteria for plasma facing materials under overall heat flow conditions of PFC. Heat transfer experiments and heat load experiments were conducted at Georgia Institute of Technology and Oak Ridge National Laboratory, respectively, in cooperation with researchers from Japan. Since those results are described in Sections 6.3 and 6.4, here we introduce an example of the results of research conducted in Japan for the purpose of supplementing the experimental results in the United States.

In conventional research on impinging jet heat transfer, the heat transfer increases as the ratio (H/D) between the nozzle-heat transfer surface distance (H) and the nozzle diameter (D) decreases. Therefore, using the experimental apparatus at GIT, with the aim of further improving the heat transfer performance, a heat transfer experiments were performed with an H/D value smaller than the HEMJ reference design value (H/D=1.0). Figure 1 shows the changes in the Reynolds number and the average Nusselt number with respect to the helium temperature when H/D=0.25 and 0.5. When H/D=0.5, the average Nusselt number increases with increasing temperature or Reynolds number. This is in agreement with the results of conventional experiments conducted at 100°C or lower. On the other hand, when H/D=0.25, when the helium temperature is 100°C or less, it exceeds the average Nusselt number when H/D=0.5, which is consistent with the previous research results. However, in the temperature range 200°C or higher, the heat transfer coefficient was lower than in the case of H/D=0.5. Furthermore, when the same H/D=0.25 was compared, there was a phenomenon that the heat transfer coefficient decreased compared to the low temperature range, which was not seen in the conventional papers. Re-laminarization is considered to be the cause of this.

Figure 2 shows the numerical simulation results of the HEMJ flow field. Focusing on the two jets on the outer circumference, when H/D=0.5, the jet structure is maintained, while when H/D=0.25, a region is formed where the symmetrical jet structure collapses and strong acceleration downstream of the jet occurs. At the outer periphery of multiple jet impingement, there may be synergistic laminarizarion caused by rapid acceleration and laminarization caused by property change of helium gas which is strongly heated near the impingement surface. This problem cannot be avoided unless the H/D value is small. It is possible to form a high acceleration region even under high temperature conditions alone, so it is important to confirm the conditions under which re-laminarization occurs and to establish the turbulence model to predict re-laminarization to realize a successful gas-cooled divertor.

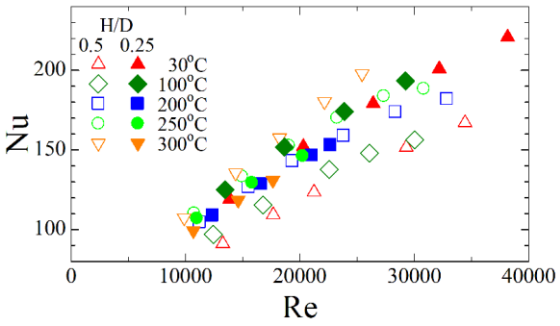

Fig. 1. Heat transfer performance degradation depending on H/D and gas temperature.

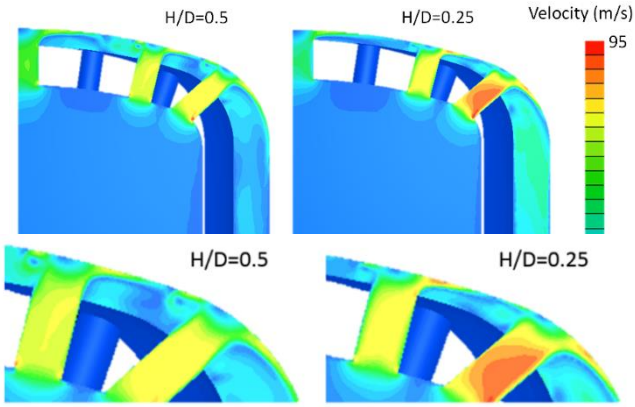

Fig. 2. Results of CFD simulation: H/D = 0.5 (left row); H/D = 0.25 (right row).

Task 2: Material Performance -Evaluation and Irradiation

Category: PHENIX
Name: T. Hinoki/A. Hasegawa/L. Garrison/Y. Katoh
Affiliation: Kyoto Univ./Tohoku Univ./ORNL

Plasma facing materials in fusion systems are exposed to very severe conditions, and neutron fluence for DEMO will be much greater than for ITER. No current commercialized materials have adequate properties to survive these conditions, especially the effects of neutron irradiation. Improved or new materials are required. Japan, the US, and other countries are devoting significant effort to material development and improvement, including increasing the fracture toughness of tungsten and other materials for use in plasma facing components (PFC). The feasibility of PFC significantly depends on material performance under thermal loads, as discussed in Task 1, among other factors. It is necessary to establish the potential and limitation of candidate materials to develop a robust design. Advanced candidate tungsten-based plasma facing materials with improved performance were selected for study in this Task. The performance of these materials under neutron irradiation was evaluated. In order to clarify displacement damage effects under lower transmutation conditions, a thermal neutron shield made of Gadolinium (Gd) was used for these irradiations in the RB*19J capsule in the High Flux Isotope Reactor (HFIR). The objective was to clarify the potential and limitations of plasma facing materials and establish a design window for a DEMO relevant divertor.

One set of materials included in the PHENIX irradiation focused on the effects of tungsten grain size, with grain size ranging from single crystal tungsten with very large grains, powder metallurgy produced tungsten with medium grains, and rolled tungsten foil with very small grains. This irradiation of unalloyed tungsten concentrated on gathering baseline irradiation data on tungsten at transmutation rate to dpa ratio that is relevant for fusion. Only very limited data existed previously on neutron irradiated tungsten at conditions similar to those expected in fusion reactors. The PHENIX collaboration collected a wide range of microstructural, thermal, and mechanical properties data for the materials [1].

Single crystal tungsten samples were included in the RB*19J capsule irradiation for direct comparison with previous irradiation of single crystal tungsten without shielding. It was noted that tungsten irradiated in HFIR without shielding undergoes high rates of transmutation to Re and Os, which leads to the precipitation of Re and Os rich clusters, with severe consequences on mechanical properties [2, 3]. The single crystal tungsten irradiated in the RB*19J shielded capsule had noticeably lower hardness after irradiation than the irradiated unshielded tungsten, which is attributed primarily to the reduced transmutation in the shielded samples. Additionally, the single crystal tungsten irradiated in the shielded capsule at the highest temperature of ~994°C has the complimentary effects of lower transmutation and higher irradiation temperature and thus more dynamic annealing of irradiation defects, leading to a lower hardness (**Error! Reference source not found.**).

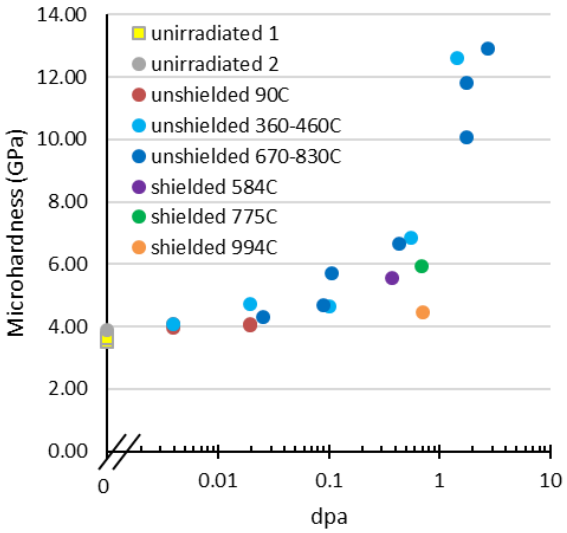

Figure 1. Microhardness of single crystal tungsten irradiated in HFIR. Temperatures listed in the legend are the average irradiation temperature of the specimens tested.

ITER W diverter tiles are fabricated by powder metallurgy, to give homogeneity to the material and limit the manufacturing cost. One feature of W or W alloy materials manufactured by powder metallurgy is control of the working ratio and the grain size. In particular, a layered structure of pancake-shaped grains is formed by rolling during the manufacture. The elastic strain due to the rolling is moderated by a stress relief heat treatment (SR) where the worked dislocations are partially recovered to form a dislocation cell structure in the grain[4, 5]. These microstructure controls can be effective in suppressing the low temperature embrittlement. In addition, potassium (K)-doping or the combination of K-doping and 3%Re addition can increase the recrystallization temperature and the high temperature strength at 1000 ˚C or higher[6, 7]. Grain refinement by K-doping and 3%Re addition is also expected to improve the low temperature embrittlement. Effects of Re addition are known to decrease the DBTT and increase high temperature strength by the solid solution strengthening mechanism[8].

Figure 2 shows engineering stress-strain curves from 700°C tensile tests of unirradiated and irradiated pure W (SR) and its alloys (SR). HFIR irradiations were at ~800°C[9]. All irradiated W materials (SR) showed yielding stress about twice that of unirradiated materials. All W materials (SR) exhibited yielding but irradiated pure W (SR) and irradiated

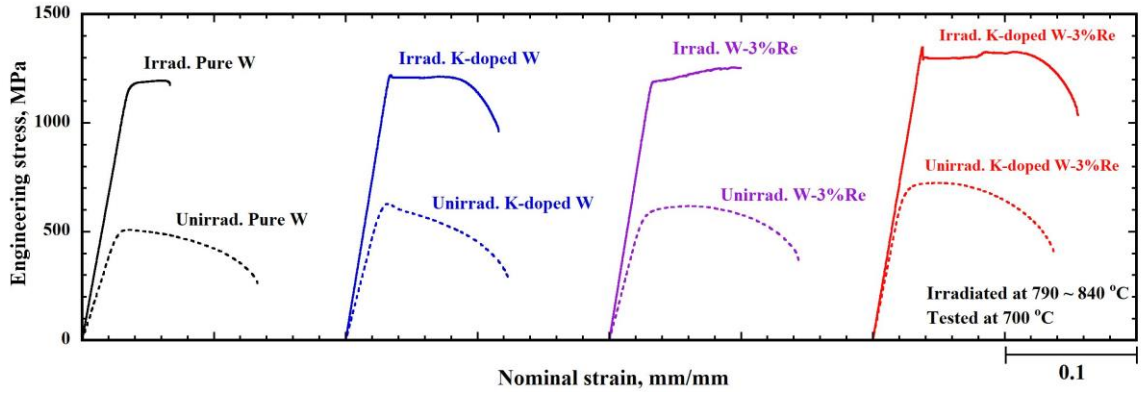

Figure 2. Engineering stress-strain curves from 700 ˚C tensile tests of unirradiated and irradiated stress relieved pure W (SR) and its alloys (SR) at 800 ˚C.

W-3%Re (SR) fractured without necking whereas irradiated K-doped W (SR) and irradiated K-doped W-3%Re (SR) fractured after a significant amount of necking. Irradiated pure W (SR) showed yielding but the elongation was reduced after irradiation compared to the unirradiated materials. The rupture surface showed no necking, with a cleavage fracture. Irradiated W-3%Re (SR) also showed the same tensile and fracture behavior as irradiated pure W (SR). Irradiated pure W (SR) and W-3%Re (SR) both showed the loss of ductility and a brittle fracture mode. On the other hand, elongation of K-doped W (SR) and K-doped W-3%Re (SR) after irradiation was almost the same as the unirradiated materials. The ruptured surfaces showed necking and dimples. Delamination of the layered structure was also observed. The results showed that K-doped W (SR) and K-doped W-3%Re (SR) had good ductility after irradiation. All W materials (SR) irradiated at 550 ˚C and evaluated at 500 ˚C also showed yield stress about twice that of unirradiated material. The irradiated pure W (SR) showed irradiation hardening and was ruptured in the elastic region without yielding. K-doped W (SR) showed yielding but a small elongation of 0.4%. However, W alloys with the addition of 3% Re (W-3%Re (SR) and K-doped W-3%Re (SR)) showed some elongation. The relevant fractographs showed necking and dimples, evidence of a ductile fracture. Delamination of the layered structure was also observed in the fracture surface in K-doped W-3%Re (SR). W alloys with the addition of 3% Re also showed irradiation hardening, but they exhibited ductility and plastic instability.

The thermal properties of tungsten are critical to its use in fusion reactors, so this was another experimental focus of the PHENIX collaboration. A special effort was devoted to developing a reliable technique for measuring the thermal diffusivity of 3 mm diameter, 0.5 mm thick miniature irradiated samples. Specimens with this geometry are more sensitive to surface condition and the fixture in the thermal diffusivity measurement device than more standard 10 mm diameter samples [10]. This effort was coordinated with the Task 1 high heat flux exposure of irradiated samples, which compared unalloyed tungsten with K-doped W-3%Re material. Thermal diffusivity was measured from room temperature to 800°C. At all temperatures the unalloyed tungsten had significantly higher thermal diffusivity than the K-doped W-3%Re, however that difference became less at higher temperatures. After irradiation in the RB*19J capsule, both materials had decreased thermal diffusivity, but the unalloyed and irradiated tungsten values still remained higher than the unirradiated K-doped W-3%Re. This confirms that the transmutation in the shielded capsule was less than 3% Re.

References

1) L.M. Garrison, et al., Fusion Science & Technology, 75 (2019) 499-509
2) L.M. Garrison, et al., Journal of Nuclear Materials, 518 (2019) 208-225
3) T. Koyanagi, et al., Journal of Nuclear Materials, 490 (2017) 66-74
4) K. Sasaki, et al., Journal of Nuclear Materials, 461 (2015) 357-364
5) K. Sasaki, et al., Fusion Engineering and Design, 88-9-10 (2013) 1735-1738
6) K. Tsuchida, et al., Nuclear Materials and Energy, 15 (2018) 158-163
7) M. Fukuda, et al., Fusion Engineering and Design, 89 (2014) 1033-1036
8) E.M. Savitskii, et al., Metal Science and Heat Treament of Metals, 2 (1960) 483-486
9) T. Miyazawa, et al., Journal of Nuclear Materials, 529 (2020)
10) M. Akiyoshi, et al., Fusion Engineering and Design, 136-Part A (2018) 513-517

Task 3: Irradiation Response on Deuterium Retention in Unshielded Neutron-Irradiated Tungsten

Category: PHENIX Task 3
Name: M. Shimada[a,*], D.A. Buchenauer [b], Y. Hatano[c], and Y. Oya[d],
Affiliation: [a]INL, [b]SNL-CA, [c]Univ.of Toyama, and [d]Shizuoka Univ.

One of the critical challenges during long-term operations of the fusion pilot plant and demonstration (DEMO) reactors is the development of fusion materials that can withstand the extreme conditions created by high plasma/neutrons particle fluxes and high heat-flux, while minimizing in-vessel inventories and ex-vessel permeation of tritium. Understanding irradiation effects on heat transfer, thermo-mechanical properties, and tritium retention/permeation in PFCs determines the feasibility and safety of divertor components under severe conditions from plasma/neutron particle fluxes and heat-flux. During the previous US-Japan TITAN program, polycrystalline tungsten (PCW) was irradiated in unshielded capsules at *low temperature* (<373K) to understand the fundamental deuterium migration and trapping mechanisms in irradiated tungsten [1]. The scope of US-Japan PHENIX Task 3 was to improve understanding of tritium behavior (retention and permeation) in tungsten and tungsten alloys under divertor-relevant high-flux plasma and *elevated temperature* regions (>873K). Approximately 300 tungsten discs (6 or 10 mm OD, and 0.25, 0.5, or 1.0 mm thickness) were irradiated at three temperature zones, nominally 773, 1073, and 1373K, to radiation level of approximately 0.5 dpa in HFIR-RB* with gadolinium neutron shielding under the PHENIX program. The Tritium Plasma Experiment (TPE) at INL offers a radiological capability to investigate irradiation effects on deuterium retention in low-activity samples. The following are highlights of irradiation response on deuterium retention in unshielded tungsten under the PHEXNIX program.

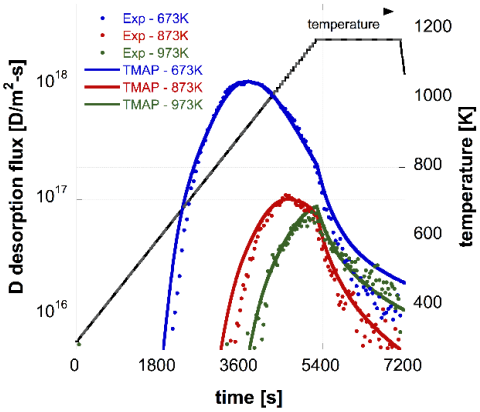

Fig. 1: The experimental TDS spectrum (in dotted line) and the TMAP-simulated TDS spectrum (in solid line) of 673 K (in blue), 873 K (in red), and 973 K (in green).

For the unshielded PHENIX program neutron irradiations, single crystal tungsten (SCW) was irradiated at elevated temperatures (633 K, 963 K, and 1073 K) to approximately 0.1 dpa in unshielded capsules to study the irradiation response. A pair of neutron-irradiated tungsten specimens was then exposed to a deuterium (D) plasma to ion fluence of 5.0×10^{25} m^{-2} at three different exposure temperatures (673 K, 873 K, and 973 K) at the TPE [2-3]. A combination of thermal desorption spectroscopy, nuclear reaction analysis, and rate-diffusion modeling code (Tritium Migration Analysis Program, TMAP) were used to understand D behavior in neutron-irradiated tungsten [2-3]. Fig. 1 shows the experimental TDS spectra of 673 K (in blue), 873 K (in red), and 973 K (in green) along with the TMAP-simulated TDS spectra for three temperature cases. Total D retention was approximately 1.9×10^{21} m^{-2} for 0.1 dpa, 673 K. A broad D desorption spectrum from the plasma-exposure temperature up to 1173 K was observed. Trap density up to 2.0×10^{-3} Traps/W and detrapping energy from 1.80 to 2.60 eV were obtained from the TMAP modeling [2-3]. Fig. 2 compares total D retention in 0.1 dpa neutron-irradiated SCW (solid triangles) [2] with the previous results from 0.025 dpa (solid circles) and 0.3 dpa irradiated SCW (solid squares) [1].

Although the near-surface D concentrations decreased at elevated temperatures, the deep migration and trapping of D resulted in non-negligible D retention in unshielded 0.1 dpa SCW due to D trapping in vacancy clusters and voids. FRONTIER program tritium permeation and retention experiments in TPE with the thermal neutron–shielded tungsten discs will be reported in future work.

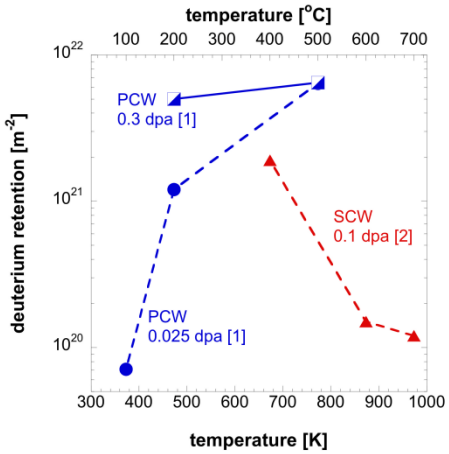

Fig. 2: Total deuterium retention from 0.1 dpa neutron-irradiated SCW (in solid triangles), and 0.025 dpa (in solid circles) and 0.3 dpa neutron-irradiated SCW (in solid square).

References:

[1] M. Shimada *et al.*, *Nucl. Fusion* **55** (2015) 013008.
[2] M. Shimada *et al.*, *Fus. Eng. Des.* **136** (2018) 1161
[3] Y. Oya *et al.*, *J. Nucl. Mater.* **539** (2020) 152323.

Task 3: Hydrogen Isotope Behavior in Irradiated Tungsten

Category: PHENIX Task 3
Name: Y. Oya, M. Shimada, Y. Hatano, D. Buchenauer
Affiliation: Shizuoka Univ., INL, Univ. Toyama, SNL

Due to the high tritium solubility in graphite, tungsten (W) is now the primary candidate material for fusion plasma-facing components. Recent studies show that tritium dynamics will be clearly controlled by the characteristics of W material, the damage profiles introduced by neutrons and other energetic particles, accumulation of impurities like He and/or C on the W surface, and transmutation of W by neutrons. The interaction of irradiation-induced defects and hydrogen isotopes is envisioned to be one of the most prominent problems for plasma-facing materials, particularly because the neutron damage will be distributed throughout the material.

In this study, damage level dependence of D retention for 0.0003 dpa to 1.0 dpa Fe^{2+} ion irradiated W samples was initially studied. For the undamaged W, D_2 desorption stages were concentrated at lower temperatures, below 500 K. However, as displacement damage was introduced, a second desorption stage (Stage 2) was found at temperatures between 500 K and 700 K. Above 0.03 dpa, an additional desorption stage (Stage 3) was found at a temperature above 700 K. The desorption temperatures for both Stages 2 and 3 shifted upward as damage was accumulated. The hydrogen isotope diffusion and trapping (HIDT) simulation revealed that the D_2 desorption behavior can be accurately simulated using three trapping sites with energies of 0.65 eV, 1.25 eV and 1.55 eV, corresponding to the desorption of D trapped by dislocation loops, vacancies and voids, respectively. Figure 1 shows the comparison of D_2 TDS spectra for W samples damaged by Fe^{2+} irradiation, by fusion neutron irradiation or by fission neutron irradiation. Although high vacancy and void concentrations within the shallow region near the surface were introduced by Fe^{2+} irradiation, single vacancies with low concentrations were distributed throughout the sample for 14 MeV neutron irradiated W. Only dislocation loops were introduced by fission neutron irradiation at low neutron fluence. The desorption peak of D for fission neutron irradiated W was concentrated in a low temperature region below 550 K, but that for 14 MeV neutron irradiated W was extended toward the higher temperature side due to D trapping by vacancies.

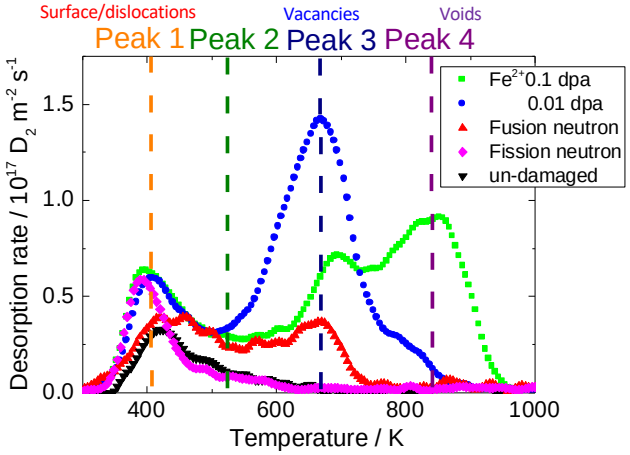

Fig. 1 Comparison of D_2 TDS spectra for irradiated W after1 keV D_2^+ implantation with 1.0×10^{22} D m^{-2}. (Fusion neutron: ~2 x 10^{-7} dpa, Fission neutron: ~4 x 10^{-4} dpa).

The effect of damage introduction at higher temperature on D retention in Fe^{2+}-irradiated W was also studied. Figure 2 shows D_2 TDS spectra for W Fe^{2+}-irradiated W at various temperatures to 0.1 dpa with Fe^{2+} and for material irradiated at room temperature then annealed at elevated temperatures. A clear reduction of D desorption at ~ 800 K after higher temperature irradiation was found compared to with W post-irradiation-annealed at that same temperature. In addition, D_2 desorption temperatures shifted toward lower temperatures for peaks at 573 K and 873 K. These results show that dynamic recovery of damage is enhanced by higher temperature irradiation, and modification of trapping sites reduces the associated trapping strength of voids.

It can be seen that the type of trapping sites and their distributions clearly controls the D desorption behavior. Accumulation of damage in W creates stable trapping sites (vacancy and voids) for hydrogen isotopes, leading to the D desorption at higher temperatures.

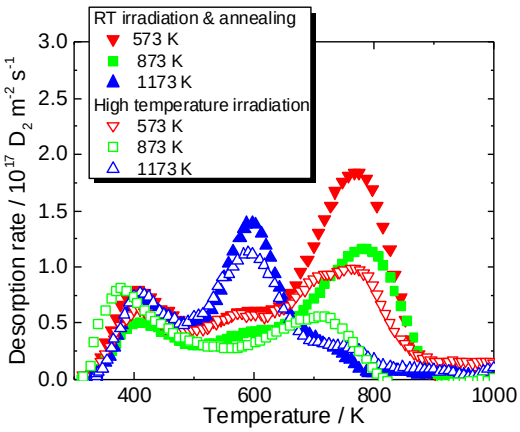

Fig. 2 D_2 TDS spectra for 0.1 dpa Fe^{2+}-irradiated W at various annealing temperatures. (1 keV D_2^+ with 1.0×10^{22} D m^{-2}).

The PHENIX Instrumented HFIR RB 19J Experiment

Category: PHENIX
Name: J.W. Geringer[1], J.M McDuffee[1], T. Hinoki[2]
Affiliation: [1]ORNL, [2]Kyoto University

The HFIR RB19J irradiation experiment was a shared collaborative effort between the US and Japan Fusion Materials programs to evaluate neutron irradiation effects in tungsten (W) for plasma facing components under divertor conditions and in blanket structural materials for DEMO and other fusion reactors. The focus of the PHENIX program was to establish effects in tungsten of fusion-relevant transmutation-to-dpa ratio to enable comparison with previous unshielded irradiations.

The experiment was designed to irradiate tungsten and RAFM (F82H) steel specimens at controlled temperatures of 300°C, 500°C, 800°C and 1200°C in the Removable Beryllium (RB) position of the High Flux Isotope Reactor (HFIR), shown in Fig. 1. The RB region is part of the reflector which is the concentric ring surrounding the control plates and outer fuel element.

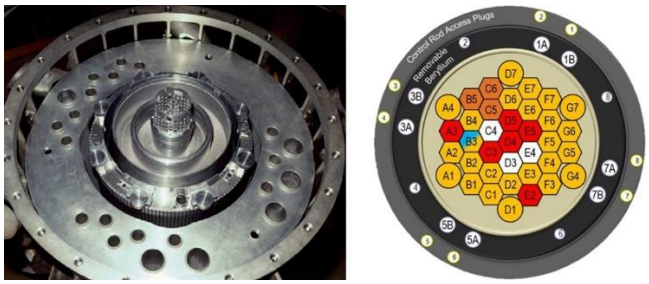

Fig. 1. The HFIR core with the beryllium reflector (left) and schematic of the RB layout (right)

The RB19J capsule contained a 1 mm thick gadolinium (Gd) metal liner, located on the inside of the capsule housing, surrounding the specimen holders. It served as a thermal neutron shield to modify the fast/thermal neutron ratio over the life of the experiment, thus controlling the W to rhenium (Re) and osmium (Os) transmutations. This was the first use of a Gd shield in the HFIR for this purpose.

The experiment contained six cylindrical holders (four temperature zones) which housed ~1300 tungsten and steel specimens. Three of the six holders were made of graphite with target temperatures of 800°C, 1200°C and 500°C and contained a variety of tungsten material specimens, including tensile, fracture toughness, torsion, various disc type specimens and even some fiber specimens. The remaining three holders were made of aluminum for a 300°C target temperature and housed the steel specimens. The effective total internal sub-capsule length was 480 mm with a mean diameter of ~30 mm.

Temperatures inside the capsule were controlled by a combination of gas gap thickness and gas composition (helium and argon) and monitored by thermocouples as shown in Fig 2. Temperature control was performed by purging the capsule with helium and then changing with a controlled gas ratio (argon-helium mixture). Passive SiC temperature monitors were included in each holder and neutron dosimetry monitors were inserted in the spacer regions between the holders.

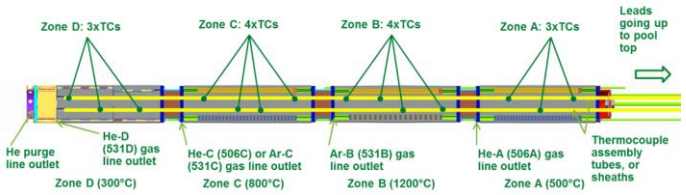

Fig. 2. Schematic of the RB19J capsule layout showing the four temperature zones and gas lines.

Assembly of the RB19J capsule was completed in May 2016 and its first HFIR irradiation cycle, 466, started in June 2016. Starting temperatures stabilized within design ranges for the 500°C and the 800°C holders. The 1200°C and the 300°C were lower and higher than designed by about 50°C and 100°C respectively. The fourth and last irradiation cycle, 469, was completed in December 2016.

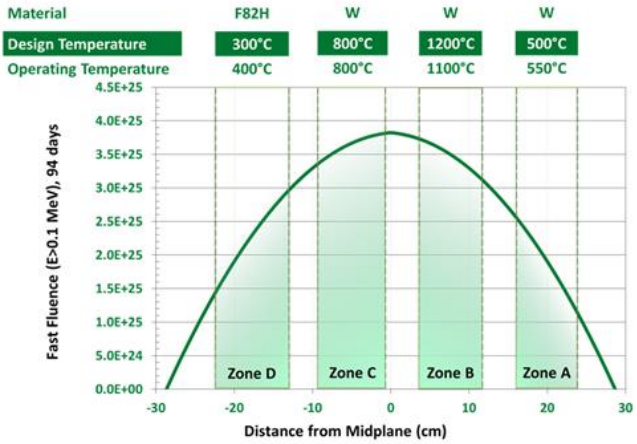

Fig. 3. Calculated fluence distribution and temperature zones over the length of the capsule.

The experiment completed a total of 8001 MWD of neutron irradiation over a period of 94 days during 4 HFIR cycles. Analysis indicated that the Gd-shield was effective during the irradiation period. Fig. 3 shows the calculated fast fluence (E > 0.1 MeV) over the four temperature zones and labels give the average temperature performance during operation.

Calculations based on post irradiation evaluation of flux monitors determined that a maximum dose of 0.586 dpa was achieved for the tungsten specimens. Analysis of the temperature monitors concluded mean temperatures of ~568°C, 848°C and 974°C for the applicable zones in the final irradiation cycle.

FRONTIER Project

Category: FRONTIER
Name: Y. Hatano[1], D. Clark[2], T. Yokomine[3], Y. Katoh[4]
Affiliation: [1]Univ. Toyama, [2]USDOE, [3]Kyoto Univ., [4]ORNL

FRONTIER is the abbreviation of Fusion Research Oriented to Neutron Irradiation Effects and Tritium Behavior at Material Interfaces. This six year project started in April 2019 with the goal of providing the scientific foundations for reaction dynamics in interfaces of plasma facing components (PFCs) for DEMO reactors.

In the TITAN (2007-2012) and PHENIX (2013-2018) projects, extensive efforts were made for the development of materials resistant to neutron irradiation and plasma exposure, joining techniques for those materials and the evaluation of hydrogen isotope retention and permeation. However, the effects of neutron irradiation on the properties of joining interfaces and hydrogen isotope transport through the interfaces have been scarcely studied. Performance and robustness of plasma-facing components might be limited by properties of those of interfaces if the properties are poorer than those of the bulk materials.

Liquid divertors may have larger heat removal capacity than W-armored solid divertors and hence that is one of the alternative options for the DEMO divertor. The compatibility of liquid metals and structural materials is an issue for liquid divertor and has been studied under static and flowing conditions. However, the effects of neutron irradiation on the compatibility have not been evaluated.

Based on these considerations this project will tackle the issues listed below:

(1) Reactions at the interface between plasma-facing materials and structural materials, the neutron irradiation effects on the reactions, and the influence of reaction layers on the mechanical properties and heat transfer of the interface;
(2) Tritium transport through the interfaces and the neutron irradiation effects;
(3) Oxidation of neutron-irradiated plasma-facing materials and subsequent tritium release; and
(4) Compatibility of liquid metals with structural materials, surface oxide films and coating materials, and neutron irradiation effects on this compatibility.

To reach these goals, four tasks were defined for the project, and are shown in Fig. 1.

The objectives of Task 1, Irradiation Effects on Reaction Dynamics at Plasma-Facing Material/Structural Material Interfaces, are to understand neutron-induced microstructure modifications and the consequent changes in mechanical and heat transfer properties of interfaces between plasma-facing material and structural material (Fig. 2). This task performs neutron-irradiation in the High Flux Isotope Reactor (HFIR) and post-irradiation examinations in the Low Activation Materials Development and Analysis laboratory (LAMDA) at Oak Ridge National Laboratory (ORNL). Task 1 has prepared a variety of layered and joined materials using state-of-the-art joining techniques such as diffusion bonding of W materials with reduced activation ferritic/martensitic steels (RAFS), Cu alloys, SiC, oxide dispersion strengthened (ODS) alloys and vanadium alloys. Direct diffusion bonding of SiC to W was successfully developed and additional focus is now on developing K-doped W laminated composites. Direct brazing between W and ODS-Cu alloy was developed. Additional underwater explosive welding and vacuum plasma spraying with friction stir processing are being explored. Composite laminates and particle reinforced W alloys are also under development. Spark plasma sintering (SPS) processing, used to develop the dispersion-strengthened W materials, was found to be useful to fabricate dense and fine-grained samples of various compositions. Based on these results, the task has established a test matrix for neutron-irradiation campaign. The design of irradiation capsules is nearly complete, and neutron irradiations will starts Japanese fiscal year 2020.

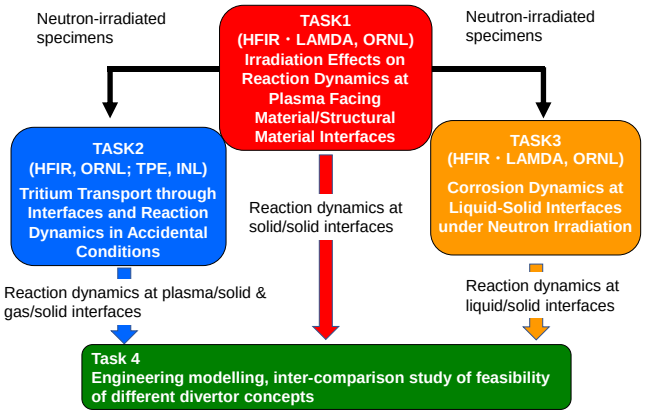

Fig. 1 Task structure of the FRONTER project.

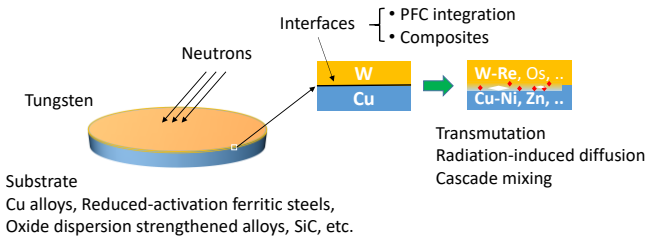

Issues: integrity, thermal conductivity, tritium transport, etc.

Fig. 2 Schematic description of neutron irradiation effects on interface between plasma-facing and structural materials.

Task 2 (Tritium Transport through Interfaces and Reaction Dynamics in Accidental Conditions) aims to measure retention and permeation of hydrogen isotopes including tritium in layered materials using the linear plasma machine Tritium Plasma Experiment (TPE) at Idaho National Laboratory (INL) (Fig. 3). In these experiments, the hydrogen isotope transport through the interface between plasma-facing material and structural material before and after neutron irradiation will be studied together with the effects of He seeding and isotope mixing in the plasma. The task also investigates the oxidation of neutron-irradiated W materials by steam, air etc. after exposure to tritium plasma. This will help construct a fundamental database on radioisotope emission from W under accidental conditions. The mobilization device built in the Safety and Tritium Applied Research (STAR) facility, INL during the JUPITER-II project (2001-2006) is available for this purpose.

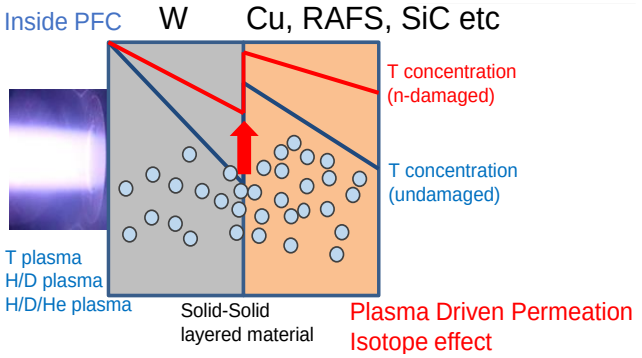

Fig. 3 Schematic diagram of tritium transport through layered materials under plasma exposure

The objective of Task 3 (Corrosion Dynamics at Liquid-Solid Interfaces under Neutron Irradiation for Liquid Divertor Concepts) is to study the corrosion characteristics of liquid Sn as a divertor coolant with and without neutron irradiation. Liquid Sn has been selected as a candidate liquid metal for divertor applications due to the acceptably low vapor pressures at expected service temperatures. Material issues for the liquid Sn divertor concept are summarized in Fig. 4. The preliminary corrosion tests of unirradiated materials under static conditions performed by the task partners revealed that Al-rich steels (e.g. Fe-15Cr-6Al steel and its ODS steel) have excellent corrosion resistance against liquid Sn. Hence, the task plans to investigate the corrosion resistance under non-isothermal conditions using a thermal convection loop at ORNL. The tube material of the thermal convection loop is AMPT steel (Fe-21Al-5Al-3Mo) and the contamination of liquid Sn by the

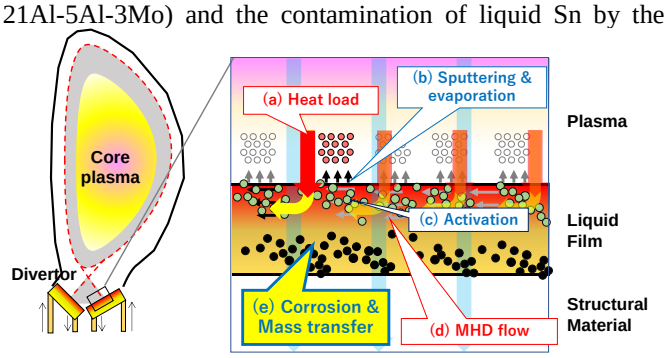

Fig. 4 Schematic diagram of a liquid divertor.

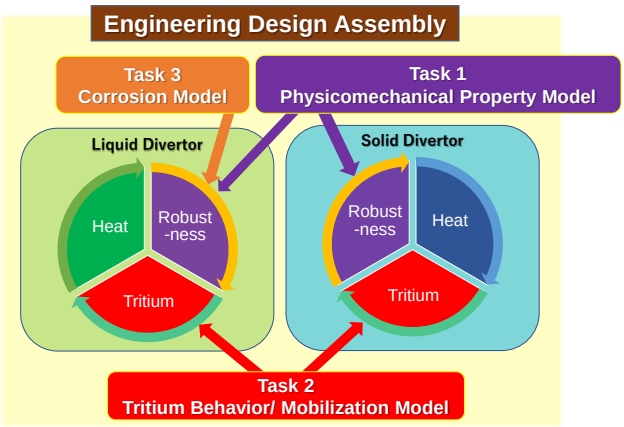

Fig. 5 Contribution of tasks in engineering modeling performed in Task 4.

corrosion of loop tubes is suppressed. The material compatibility test under neutron irradiation in HFIR is also under planning. In the current capsule design, two SSJ specimens are installed in a single capsule together with a small amount of liquid Sn.

Task 4 (Engineering Modeling) will consolidate the results of each task focusing on hetero-phase/interphase interfacial dynamics interdisciplinary, link them organically as a phenomenon acting in the PFCs, and apply to an engineering model that can correspond to the PFC system (Fig. 5). At present, a system with water cooling and W material is the main candidate divertor concept, but resistance to unexpected large heat loads is low. Against this backdrop, the task conducts an engineering inter-comparison study of gas-cooled solid divertor and liquid divertor to evaluate their relative feasibilities.

CHAPTER 7 HFIR Collaborative Research

Japan and the United States have worked together for 36 years on a Project between JAERI, JAEA, then QST, MEXT of Japan, and U.S. DOE. This Collaboration is now under the Cooperation in Research and Development in Energy and Related Fields. Both partners note with satisfaction the steady progress and high productivity of this partnership and look forward to the continuation and growth of this collaboration.

7.1 Objectives

The goal of this collaboration is to jointly design, conduct, and evaluate irradiation experiments in the High Flux Isotope Reactor (HFIR) at Oak Ridge National Laboratory to investigate the irradiation response of structural materials that are of interest to Japan and U.S. The final objective of this collaboration is to develop and qualify structural materials for use in fusion reactors.

Two classes of properties are evaluated to establish the performance limits of materials – (1) the basic properties needed to identify the mechanisms that control the degradation of performance under irradiation, and (2) the engineering properties that contribute to the database needed for DEMO reactor design. This knowledge of the material behavior is combined with the available comprehensive modeling efforts to extrapolate behavior beyond the database to reactor operating conditions and to identify promising paths for compositional or microstructural modifications that will lead to improved material systems.

7.2 Accomplishments and Highlights

The collaborative testing program for fusion first wall and blanket structural materials (FSM) has completed seven phases, each of five-year terms, in the program starting in 1983. The current Phase VIII of this collaborative program (FSM-P8) started in April 2019.

In the last 10 years, HFIR target position experiments JP-28, -29, -30, and -31 completed irradiation, reaching DEMO-relevant goal maximum exposures of 80 and 20 dpa at the

irradiation temperature from 300 to 500 °C on Japanese RAFM steel F82H variations, including Ni-doped F82H to simulate transmutation formed He production under fusion neutron irradiation, and U.S. advanced nanostructured ferrite alloys. The companion HFIR target position rabbit capsules also achieve the goal fluences of 50 and 20 dpa on F82H variations at 300°C. The tensile properties after these high dose irradiations at a lower temperature (~300°C) show the largest hardening and loss of total elongation compared to the lower dose (<30dpa) results but did not show complete embrittlement. Fracture toughness of ~70dpa irradiated F82H, and its variation is the world's first toughness data of Reduced Activation Ferritic/Martensitic (RAFM) steel. It revealed that F82H MOD3, the toughness-improved version of F82H, shows it has better toughness, preserved even after irradiation. Results on irradiated 58Ni-doped F82H, which contained ~770 appm He, might indicate a potential detrimental He effect on fracture toughness.

Several rabbit capsules with SiC specimens have completed irradiation in HFIR to 40, 70, and 100 dpa, while other high fluence capsules continue irradiation in the reactor to target fluences up to 200 dpa. The results obtained to date indicate no evidence of irradiation-induced mechanical property degradation or progressive radiation damage in high purity SiC in stoichiometric and polycrystalline form. This indicates there is significant room for improvement in high dose radiation tolerance of the commercial SiC-based nanocrystalline fibers and pyrolytic carbon interphases used in the current generation nuclear grade SiC/SiC composites. These very high dose neutron irradiation campaigns for SiC ceramics and composites are unique to this DOE-QST HFIR collaboration, making it a world-leading program that is generating the data required in evaluating these materials for use in fusion power reactor in-vessel components.

Two HFIR removable beryllium (RB*) position experiments, capsules designed with instrumentation and sweep gas flow for temperature control, have completed irradiation. RB15J, which had a europium thermal neutron shield for neutron spectrum tailoring, achieved 6 dpa exposure of F82H, F82H weld joints, and B-doped F82H at 300 and 400°C. The results of specimen evaluation indicated that the tendency for localized deformation at

the heat-affected zone (HAZ) of weldment became significant after irradiation, but that this tendency does not appear if the volume fraction of HAZ is near zero or very small. Irradiation creep was evaluated using pressurized creep tubes; and ^{10}B-doped F82H, which generated ~300 appm He, showed a slightly larger creep strain compared to that of ^{11}B-doped F82H, and the estimated swelling level expected from the formation of small helium bubbles in the ^{10}B-doped material is consistent with the difference measured in creep strain.

A shared HFIR irradiation experiment, the RB19J with a gadolinium thermal neutron shield, has completed irradiation and achieved a maximum of 2.5 dpa exposure on F82H alloy variations. The SiC temperature monitors indicated that most of the specimen were irradiated at a higher temperature than the design temperature, but the bottom section specimens indicated the smallest deviation. Those specimens will be tested in the near future.

A new program of collaborative HFIR irradiation and examination of fusion reactor structural materials for DEMO design activities (DDA) was started in April 2018, and Phase I of the collaborative program (DDA-P1) is now underway. The first campaign of HFIR rabbit capsule irradiation of Cu alloys, candidate structural material for divertors, was completed in 2020. The results will contribute to the expansion of the DEMO irradiation effects database.

During the period 2010 to 2019, 24 Japanese scientists visited ORNL for direct collaboration on post-irradiation experiments and to assist in preparing irradiation experiments in collaboration with U.S. scientists. In that same period 30 papers based on the collaborative work were published. The results and direction of this collaboration, including the personnel and technical exchanges, continue to be of value to both Japan and the U.S. and of interest and value to the international fusion community. Steady progress in improving material performance and in understanding the effects of the fusion environment on material properties can be seen throughout this long and productive collaboration

Effect of High-Dose Neutron Irradiation on the F82H RAFM Steel

Category: FTPC
Name: T. Hirose, H. Tanigawa, H. Sakasegawa, M. Ando, / Y. Katoh, X. Chen, J.W. Geringer, L. Tan, B.K. Kim, K.G. Field, L.L. Snead
Affiliation: QST/ORNL

The reduced activation ferritic/martensitic (RAFM) steel F82H was irradiated up to 87 dpa at 573, 673 and 773 K in the High Flux Isotope Reactor (HFIR) at Oak Ridge National Laboratory, which took seven years to complete irradiation. The materials examined in this work are reduced activation ferritic/martensitic steel, F82H-IEA (0.1C-8Cr-2W-0.2V-0.04Ta) and F82H with additional tantalum added for toughness improvement, F82H-MOD3 (0.1C-8Cr-2W-0.2V-0.09Ta)[1]. Preliminary analysis of the passive thermometry demonstrated it was possible the irradiation temperature was lower than the design temperature, especially for specimen holders intended for 673 and 773 K[2].

Tensile tests of the irradiated miniature dog bone specimen, SS-J3, were conducted at the nominal irradiation temperatures[3]. Tensile properties of F82H-MOD3 were comparable with those of F82H-IEA, and showed obvious irradiation hardening even above 673 K for all specimens. Most irradiated specimens had poor elongation less than 10 % at the test temperature.

The dose dependence of hardening as the 0.2% proof stress and total elongation are given in Figure 1 and Figure 2, respectively. These figures include previous results from material irradiated in the Fast Breeder Reactors (FBRs) Fast Flux Test Facility (FFTF)[4] and BOR-60[5]. Irradiation hardening at 573 K asymptotically increases to 500 MPa, and seems to be consistent with the previous work in FBRs. In contrast, the hardening gradually increased with increasing dose for HFIR irradiation at temperature above 663 K where softening was observed in FBRs experiments. It is noted that F82H irradiated in the FFTF tended to show increased hardening to doses from 40 to 60 dpa. Therefore, hardening at higher temperature might have an incubation dose for hardening to start.

As shown in Figure 2, the dose dependence of ductility changes seems to be strongly affected by specimen geometry. Specimen with lower aspect ratio demonstrated a tendency for saturation of total elongation around 7%. In contrast, modified specimens with larger aspect ratio, SS-J3, successfully evaluated a gradual decrease of total elongation. We did not see any obvious tendency for saturation in loss of ductility in this work.

Irradiation conditions in HFIR and FFTF experiments are different in damage rate, but normalized by megawatt day (MWD) are within a factor of two. Moreover, the irradiation periods are too short to demonstrate mechanical property changes due to thermal aging. Therefore, these facts imply that hardening behavior is affected by the difference in the irradiation conditions.

Calculations show that HFIR introduces 30 times larger transmutation of tungsten than does FFTF. This is due to the three order of magnitude difference in neutron flux near neutron energy of 20 eV where tungsten has a giant resonance[6]. Although it is reported that osmium and rhenium have no significant effects in martensitic steel, precipitates such as Laves phase include these elements and have strong impact on the mechanical properties[7]. This ductility loss at 673 and 773 K should be monitored as well as embrittlement since these properties might limit the use of these steels.

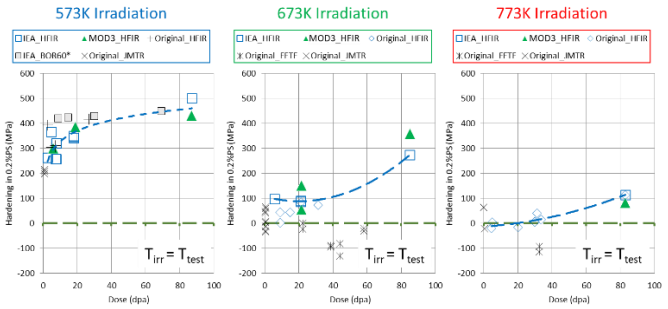

Fig. 1. Does dependence of irradiation hardening in F82H

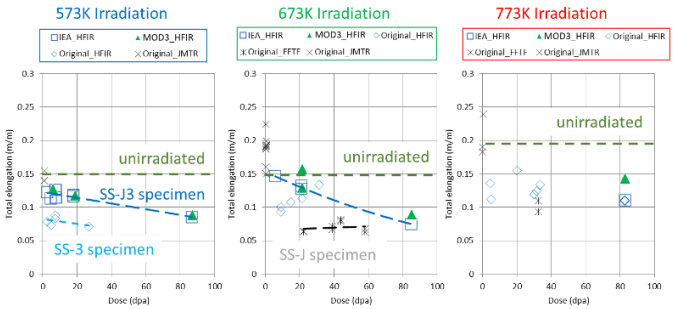

Fig. 2. Does dependence of irradiation induced ductility loss in F82H

1) K. Shiba, H. Tanigawa, T. Hirose, T. Nakata, Fusion Sci. Tech., 62 (2012) 145.
2) H. Sakasegawa, H. Tanigawa *et al.*, DOE/ER-0313 Semi-Annual Progress Reports, 59 (2015) 22
3) T. Hirose, H. Tanigawa *et al.*, DOE/ER-0313 Semi-Annual Progress Reports, 62 (2017) 8
4) Y. Kohno, A. Kohyama, *et al.*, J. Nucl. Mater. 271&272 (1999) 145
5) E. Gaganidze, J. Aktaa, Fusion Eng. Des, 88 (2013) 118
6) R.E. Stoller and L.R. Greenwood, J. Nucl. Mater. 271-272 (1999) 57
7) R.L. Klueh, D.J. Alexander, M.A. Sokolov, J. Nucl. Mater. 279 (2000) 91

Fracture Toughness of F82H Irradiated in HFIR-JP28/JP29

Category: RAFM
Name: X. Chen
Affiliation: ORNL

F82H is the reference reduced-activation ferritic-martensitic (RAFM) steel in Japan as the candidate structural material for fusion blanket applications. It has favorable properties for fusion applications such as lower radioactivity, superior swelling resistance, good thermal conductivity, and sufficient fracture toughness in the normalized and tempered condition. However, the harsh environment of a fusion reactor, such as neutron irradiation and He/H damage, can result in significant degradation of materials fracture toughness. Therefore, understanding the fracture toughness behavior of F82H in the fusion environment is critical to ensure the long-term safe operation of the fusion reactor. To address the effects of high dose irradiation and He on fracture toughness of F82H, standard and Ni-doped F82H were irradiated in the JP28 and JP29 irradiation campaigns at the High Flux Isotope Reactor (HFIR) of Oak Ridge National Laboratory (ORNL). The irradiation covered an irradiation temperature range of 300-500°C with the peak dose up to ~70 displacements per atom (dpa). This report presents the post irradiation examination (PIE) of F82H fracture toughness after 300°C irradiation.

The irradiation conditions are summarized in Table 1. Four variants of F82H, including F82H IEA, F82H Mod3, F82H doped with 1.4% ^{58}Ni, and F82H doped with 1.4% ^{60}Ni, were irradiated. Vickers microhardness and Master Curve fracture toughness testing was performed on the M3CVN miniature multi-notch bend bar specimens machined in the T-S orientation of each material.

Table 1. Irradiation conditions of F82H

Materials	Target irradiation temperature (°C)	SiC thermometry temperature (°C)	Dose (dpa)
F82H IEA	300	341	68
F82H Mod3	300	341	68
F82H+1.4 ^{58}Ni	300	307	70
F82H+1.4 ^{60}Ni	300	307	70

The post-irradiation hardness followed the order of F82H Mod3 < F82H IEA < F82H+1.4% ^{60}Ni < F82H+1.4% ^{58}Ni as shown in Fig. 1. The hardness results were in general agreement with the upper shift in the Master Curve transition temperature T_0 shown in Fig. 2 with an exception that F82H+1.4% ^{60}Ni had less embrittlement than what would have been expected from hardness measurements. Nonetheless, no detrimental effect of 1.4% ^{60}Ni doping on F82H fracture toughness was observed after neutron irradiation. F82H Mod3 was developed as a toughness-improved F82H and its better toughness was preserved even after irradiation. Significant embrittlement in irradiated F82H+1.4% ^{58}Ni which contained ~770 appm transmutation He may indicate a potential detrimental He effect on fracture toughness, but further study is needed to confirm this observation.

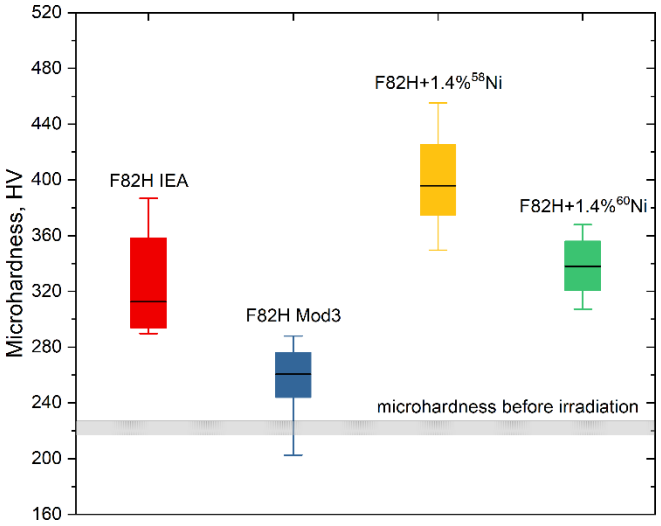

Fig. 1. Vickers microhardness of four F82H steels after irradiation. The median, ± one standard deviation, and min-max hardness measurements are shown as the horizontal line, the box, and the whisker, respectively.

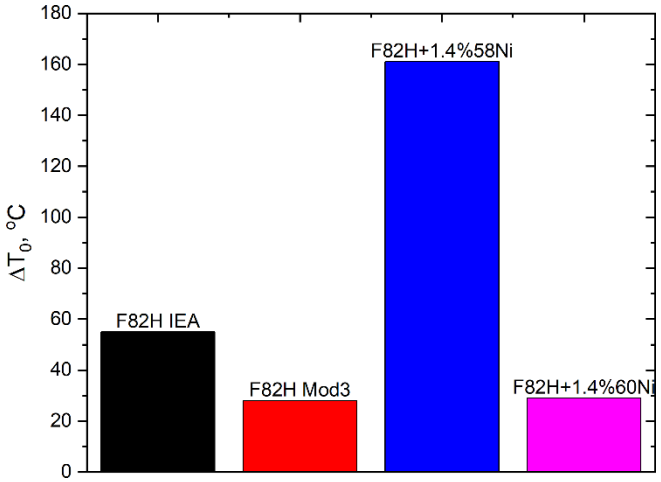

Fig. 2. Upper shift in the Master Curve transition temperature T_0 of four F82H steels after irradiation

The JP28 and JP29 irradiation campaigns for F82H steels represent the highest dose irradiation on such materials to date. Fracture toughness PIE is critical for addressing burning questions for the irradiation embrittlement behavior of F82H, e.g. the high dose embrittlement saturation behavior and the He effect on fracture toughness.

Irradiation Response of Weldments and HIP Joints in RAFM Steel, F82H

Category: FTPC
Name: T. Hirose, M. Ando, H. Tanigawa, K. Shiba/
M.A. Sokolov, R.E. Stoller / G.R. Odette
Affiliation: QST/ ORNL / UCSB

The fusion breeding blanket is an in-vessel component located around the fusion plasma that will be exposed to high heat load and neutron flux. In the Japanese reference design for DEMO, the first wall (FW) of the blanket, which faces the fusion plasma, has built-in cooling channels made by hot-isostatic-pressing (HIP). The FW is welded to the side walls (SWs) and back wall to form a box structure of the blanket. Therefore, the joints are exposed to a high neutron flux and it is necessary to investigate their response to irradiation. The objective of this work is to investigate irradiation response of the F82H joints. These sample joints were prepared by tungsten-inert-gas (TIG) welding, electron beam (EB) welding, and HIP[1].

The weld joints investigated in this work were produced from plate of 15 mm thick F82H-IEA (Fe-8Cr-2W-0.2V-0.04Ta-0.1C LN) which was hot-rolled at 1473 K and then normalized at 1313 K for 0.63 h and tempered at 1023 K for 1 h. TIG and EB weldments were annealed at 993 K for 1 h as a post-weld heat treatment (PWHT). The chemical compositions of F82H TIG weld wire was Fe-7.4Cr-2W-0.22V-0.03Ta-0.07C-LN. The specimens tested were SS-J3 sheet tensile specimens with gauge section 5 x 0.76 x 1.2 mm. In the case of the TIG welded joints the fine-grained HAZ (FG-HAZ) is defined as the HAZ heated above the AC_3 transformation temperature during the TIG welding process. Over-tempered HAZ (OT-HAZ) is defined as the zone heated below the AC_3 temperature. The HIP joint was prepared from 25 mm-thick F82H-IEA plates. HIP was conducted at 1373 K with 150 MPa for 2h using a KOBELCO O2-Dr. HIP. The HIP joint was heat treated at 1233 K for 0.5 h and 1023 K for 1 h to optimize the microstructure[2].

Neutron irradiation was conducted in the High Flux Isotope Reactor (HFIR) at the Oak Ridge National Laboratory (ORNL). The specimens were irradiated in liquid lithium in the instrumented capsule MFE-RB-15J, which used a europium thermal neutron shield for neutron spectrum tailoring. The nominal irradiation conditions were 3 and 4.5 dpa at 573 K[3]. All post irradiation tensile and Charpy impact tests, were conducted in the Irradiated Materials Examination and Testing (IMET) hot cell facility at ORNL

Post irradiation tensile tests conducted at the irradiation temperature indicated that irradiation hardening in TIG weldment and base metal was greater than 300 MPa. However, the TIG weld joint, which included a HAZ region, exhibited about half that of the F82H-IEA (equivalent to base metal: BM) after irradiation at 573 K (Fig.1). It was also revealed that the deformation tended to be localized in the HAZ section and this tendency was enhanced after irradiation. This indicates that the neutron irradiation significantly decreases the strength of the HAZ, because the HAZ is the weakest part of the joint even before irradiation.

On the other hand, the irradiation response of the HIP joint was similar to that of the base metal. Post tensile properties of the HIP joint were almost equivalent to those of base metal. Charpy impact test indicated that there was no significant drop of upper shelf impact absorbed energy in fracture behavior of the HIP interface, even though the irradiation caused embrittlement of the matrix material.

These results suggested that the weld joints could be in danger of local deformation at the HAZ, which could be found in the joint between the FW and the SWs. Thus, it would be better if the weld joint can be shifted as far away as possible from the plasma side to reduce the impact of neutron irradiation. HIP joints, which will be located in the FW, could be expected not to increase the possibility of failure, as long as the initial soundness of HIP joints can be guaranteed.

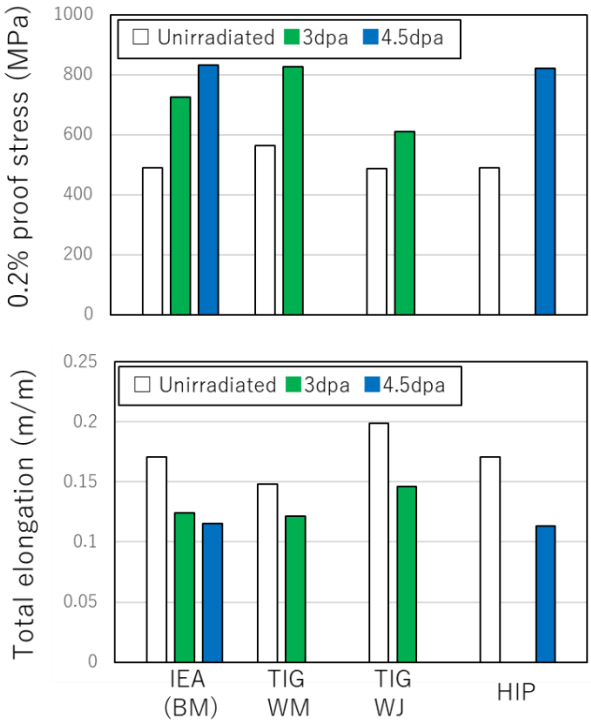

Fig. 1. Tensile properties of F82H-IEA base metal and joints irradiated at 573K. (Top) 0.2% proof stress, and (lower) total elongation

1) T. Hirose *et al.*, J. Nucl. Mater. 442 (2013) S557
2) T. Hirose *et al.*, J. Nucl. Mater. 329-333 (2004) 324
3) T. Hirose *et al.*, DOE/ER-0313 46 (2009) 72-78

Irradiation Creep of B-doped F82H Irradiated in the HFIR RB15J Capsule

Category: FTPC
Name: M. Ando, T. Nozawa, T. Hirose, H. Tanigawa / Y. Katoh
Affiliation: QST/ ORNL

Reduced activation ferritic/martensitic steels (RAFM) are the most promising candidates for blanket structural materials of fusion reactors. Irradiation creep has been recognized as one of the important properties for engineering data required for the blanket structural design. Specifically, it is anticipated that irradiation creep of RAFM at lower temperatures (<573K) could be significant for fusion reactors. Furthermore, some transmutation products (mainly helium atoms) will also be produced by high-energy neutrons in the first wall of a fusion reactor. In this research, irradiation creep data at 573-673K up to 6 dpa was successfully obtained using a liquid metal filled capsule, and the effect of helium (~300 appm) on irradiation creep behavior was examined by comparing pressurized creep tubes (PCT) of F82H and B-doped F82H.

The materials studied were F82H IEA heat (8Cr-2WVTa) and boron-doped F82H steels. The ^{10}B-doped F82H was provided to investigate the effect of helium on mechanical properties. In this experiment, two types of boron-doped F82H were prepared by a co-doping with boron and nitrogen in F82H steel[1]. The ^{10}BN-F82H produced helium atoms during irradiation by the reaction ^{10}B (n, α) ^{7}Li.; the ^{11}BN-F82H did not produce helium. The tube specimens had dimensions of 4.5 mm outside diameter and 25.4 mm length with a 0.2 mm wall thickness as shown in Figure 1.

End caps were electron beam welded to the tube segments, and the specimens were pressurized with high purity helium to obtain the desired hoop stresses at the irradiation temperatures. The hoop stresses ranged from 0 to 380 MPa at the irradiation temperature. Irradiation was performed in the HFIR to atomic displacement levels up to 5.8 dpa in the removable beryllium (RB) position. This capsule was equipped with a thermal neutron shield. As a result, ^{10}B was slowly transmuted to helium during irradiation. Nominal irradiation temperatures were 573 and 673K. Each tube was measured using a laser profilometer system in the ORNL hot cell. Irradiation creep strain was calculated from tube diameter measured before and after irradiation.

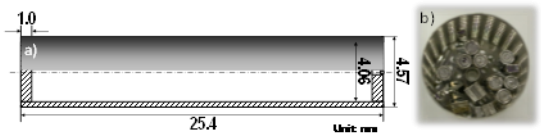

Fig. 1. a) Geometry of the PCT specimen, b) PCT specimens inside RB-15J specimen holder basket.

Figure 2a shows the relationship between the effective creep strain ($\varepsilon_{eff.}$) and the effective stress ($\sigma_{eff.}$) for F82H IEA and BN-F82H irradiated at 573K. The F82H IEA and BN-F82H exhibit similar irradiation creep behavior at 573K up to ~4 dpa. The irradiation creep strain in F82H was nearly linearly dependent on the effective stress for stresses up to ~260 MPa. However, the creep strain becomes nonlinear at higher stress levels. Figure 2b shows the results for 673K irradiation. In this case, the irradiation creep strain of F82H is linear below ~170 MPa. The effect of helium on irradiation creep of F82H was also examined by comparing ^{10}BN and ^{11}BN-F82H. Helium production during irradiation was estimated to be about 300 appm and its production rate was controlled in this thermal neutron shielded capsule. The creep strain of ^{10}BN-F82H was similar to that of F82H IEA at each effective stress level except for ~290 MPa at 573K irradiation. For 673K irradiation, the creep strain of some ^{10}BN-F82H tubes was larger than that of ^{11}BN-F82H tubes. It is suggested that a limited amount of swelling may be induced in ^{10}BN-F82H because of small helium bubbles arising from the production of helium by the ^{10}B(n, α)^{7}Li reaction. An estimated 0.06% swelling was obtained based on the volume increase of tube. This result is consistent with the swelling expected from formation of small helium bubbles.

In this research, the effect of helium on irradiation creep behavior up to 300 appm, ~6 dpa was examined using F82H and BN-doped F82H in the HFIR RB capsule. At 573K and 4.2 dpa, the irradiation creep behavior of F82H and ^{10}BN-doped F82H was similar. On the other hand, at 673K, and 5.8 dpa, the irradiation hardening and creep strain in ^{10}BN-doped F82H was slightly higher. However, they did not cause a large difference in irradiation creep behavior.

Recently, some new rabbit capsule creep experiments using PCT specimens are being developed at ORNL[2]. They will contribute to the difficult task of obtaining irradiation creep data at higher dose levels.

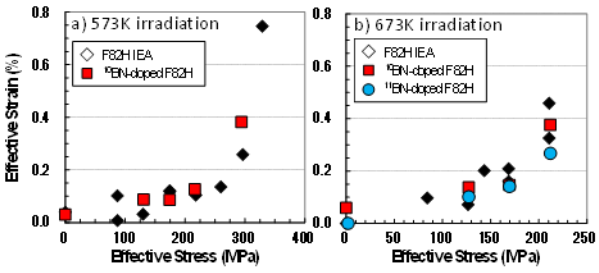

Fig. 2. Summary of irradiation creep behavior for F82H. a) 573K irradiation, b) 673K irradiation.

1) E. Wakai et al., et al., J. Nucl. Mater., 398, 64-67 (2010).
2) A. A. Campbell et al., DOE/ER-0313/67 (2019) 147-153.

Impact of Inclusions on Fracture of Irradiated RAFM Steels

Category: FTPC
Name: H. Tanigawa, M. Ando, T. Hirose, T. Kato, H. Sakasegawa/ N. Okubo / Y. Katoh
Affiliation: QST / JAEA / ORNL

Inclusions in steels, mostly oxides or sulfide formed during melting, are expected to have no significant impact on most mechanical properties as long as inclusions are controlled to low number density and do not agglomerate in a narrow region. This is because steels have enough plasticity and work-hardenability to blunt any cracks formed around inclusions and prevent further crack propagation. On the other hand, it is well known that those impacts become significant in high strength steels or high yield-tensile ratio (YR) steel. In high YR steel, the fatigue properties are sensitive to inclusions, but the tensile fracture process is also affected by the inclusions.

The reduced activation ferritic/martensitic (RAFM) F82H (Fe-8Cr-2W, V, Ta), is a relatively high YR steel (YR=~0.85), developed with an emphasis on high-temperature properties. Significant issues for RAFM steels are irradiation-induced hardening, loss of uniform elongation, and embrittlement observed after irradiation at low irradiation temperature, where YR becomes about 1 as a consequence. This suggests that the impact of inclusions on the fracture process could become significant after irradiation. This study investigates these possible impacts of inclusion on the fracture process through fractography of mechanical-tested F82H.

Typical inclusions observed in F82H were Al_2O_3, Ta_2O_5, MnS, and inclusion a mix of these 3 types. It was reported that Ta_2O_5, tends to form a large composite oxide with Al_2O_3 and tend to agglomerate at mid positions of plates, if the steel was fabricated with insufficient deoxidation[1]. For unirradiated F82H, those inclusions affect the Charpy impact properties, but have no significant effect on tensile properties.

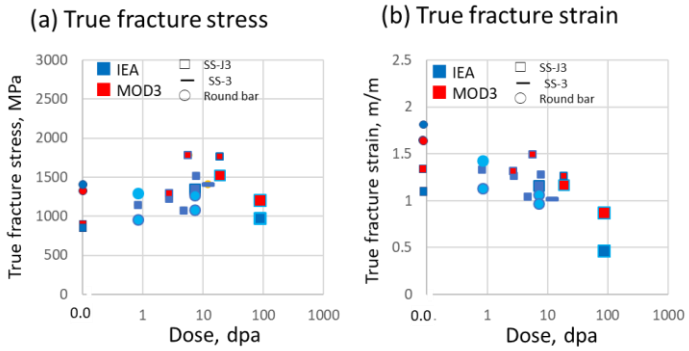

Fig. 1. Irradiation dose dependence of (a) true fracture stress and (b) true fracture strain of irradiated F82H-IEA and F82H-MOD3

Tensile properties were evaluated at irradiated temperatures on F82H-IEA (Fe-8Cr-2W-0.2V-0.04Ta-0.1C LN) and F82H-MOD3 (Fe-8Cr-2W-0.2V-0.1Ta-0.1C LN) irradiated up to 84 dpa at 300°C[2]. In these F82H variations, the large inclusions, typically composite oxides, tend to be observed in IEA, but not in MOD3. It was observed that the yield stress kept increasing, and the total elongation decreasing as the irradiation dose increase in both F82H-IEA and MOD3. The true fracture stress and strain were evaluated based on the reduction in area data, analyzed through fracture surface observation. The data suggested that the true fracture stress was not significantly affected by irradiation dose, but the true fracture strain degraded as the dose increased, and this tendency was more significant in F82H-IEA (Fig.1).

Fracture surface details were analyzed by scanning electron microscope (SEM) followed by 3D surface generation using three tilted images (Fig.2), in order to understand the mechanisms that caused the different true fracture strain degradation. These details indicated that shallower and smaller equiaxed dimples were observed on the fracture surface of heavily irradiated MOD3, but a few deep dimples with a large inclusion at the bottom were observed in irradiated F82H-IEA. These morphologies suggest that the extensive degradation of true fracture strain might be caused by the presence of larger inclusions observed in F82H-IEA, while those of MOD3 were not comparably significant.

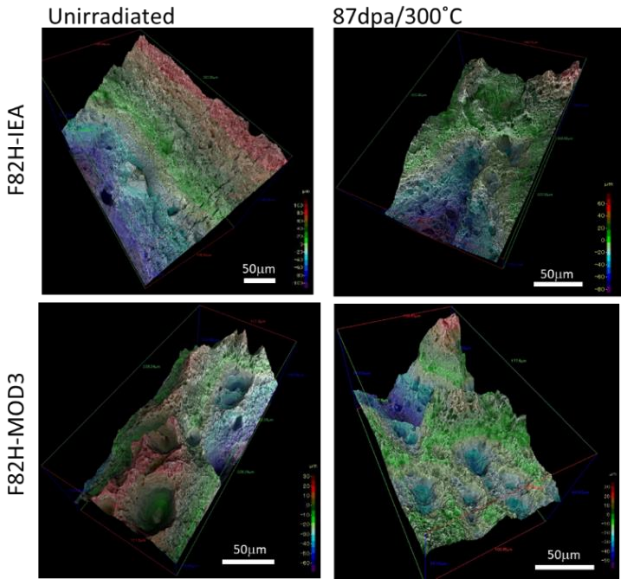

Fig. 2. Generated 3D tensile fracture surfaces of unirradiated and irradiated F82H-IEA and MOD3

1) H. Tanigawa, H. Sakasegawa, T. Hirose, Fusion Eng. & Des., 88 (2013) 2611
2) H. Tanigawa, M. Ando *et al.*, *Presented in ICFRM-17 Aachen, Germany, 11-16 October 2015*

Microstructures of RAFM Steels Irradiated to 72 dpa

Category: FTPC
Name: K. Wang*, C.M. Parish, K.G. Field, L. Tan, Y. Katoh, H. Tanigawa**
Affiliation: ORNL (*: Now at Alfred University), **QST

A reduced activation ferritic/martensitic steel, Eurofer97, was neutron irradiated up to 72 dpa near 300°C in the High Flux Isotope Reactor (HFIR). Electron microscopy was applied to investigate the radiation-induced segregation and phase instability that occurred during the neutron irradiation. Amorphization was observed in $M_{23}C_6$ carbides. Cr-rich clusters were seen within the matrix, near the lath boundaries and close to the $M_{23}C_6$ carbides. Cr enrichment and Fe depletion were detected at both prior austenite grain boundaries and lath boundaries, but differed in segregation magnitude. In addition, the enrichment of Ni, the depletion of V, and tiny cavities (presumably helium bubbles) are also found at lath boundaries. This work interrogates the evolution of microstructures during neutron irradiation, which provides detailed understanding of the microstructural aspects controlling the mechanical integrity of Eurofer97 under high-dose neutron damage.

The material used in this study was a European reduced activation ferritic/martensitic (RAF/M) steel, Eurofer97. The as-received material had a tempered martensitic steel structure, with typical lath microstructures arranged in packets within the prior austenitic grains (PAGs). The specimens were irradiated in the JP28 & 29 full-length target capsules in HFIR. The irradiation temperature was designed to be 300 °C, which was estimated to be ≈284°C based on SiC temperature monitors. The total irradiation time was 58 HFIR cycles (26,824 h), in calendar years 2005-2013. The estimated neutron fluence was 9.4×10^{22} n·cm^{-2} (E>0.1 MeV) or ≈72 dpa with the neutron flux of 9.7×10^{14} n·cm^{-2}s^{-1} (equivalent to 7.5×10^{-7} dpa·s^{-1}).

The unirradiated archive material (Fig. 1) consists of a typical F/M microstructure. Although the 72 dpa microstructure (Fig. 2) is overall similar, important differences are seen. Most significantly, large amounts of Os (a W neutron-transmutation product) are visible in the Cr-W carbides after 72 dpa but not in the archive material.

Irradiation caused significant segregation along boundaries. Both prior-austenite grain (PAG) and lath boundaries showed Fe depletion and Cr enrichment. Ni enrichment was also observed, despite very low bulk Ni content.

Further, the $M_{23}C_6$ precipitates were observed to have amorphized by 72 dpa, and small clusters of Cr were observed to have formed in halos around the $M_{23}C_6$ particles, perhaps due to a combination of diffusional kinetics and ballistic dissolution over the time to accumulate 72 dpa. Matrix Cr-rich clusters, possibly α', were also observed. Tiny cavities, presumably helium bubbles, sit at the lath boundary.

Overall, this work showed matrix phase instability and elemental segregation at the boundaries in Eurofer97 after neutron irradiation up to 72 dpa at 300 °C. PAG boundaries and lath boundaries show large elemental segregation.

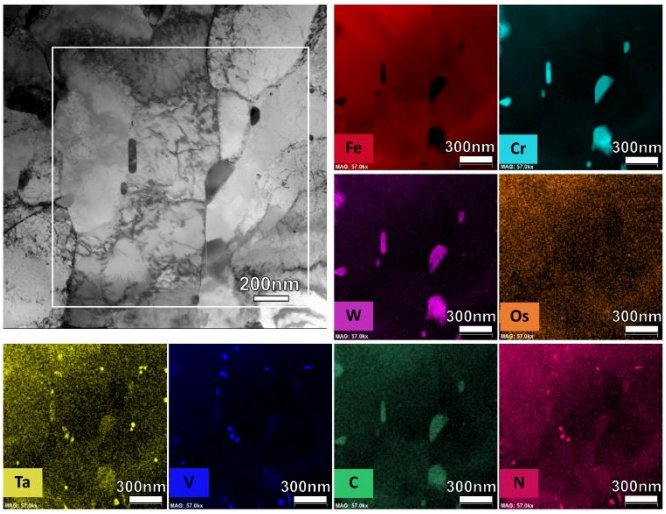

Fig. 1. Bright field (BF) TEM image of typical martensite structure of unirradiated Eurofer97 and the corresponding STEM-EDS elemental mapping results of the white rectangle region in BF TEM image. 3×3 pixel smoothing applied.

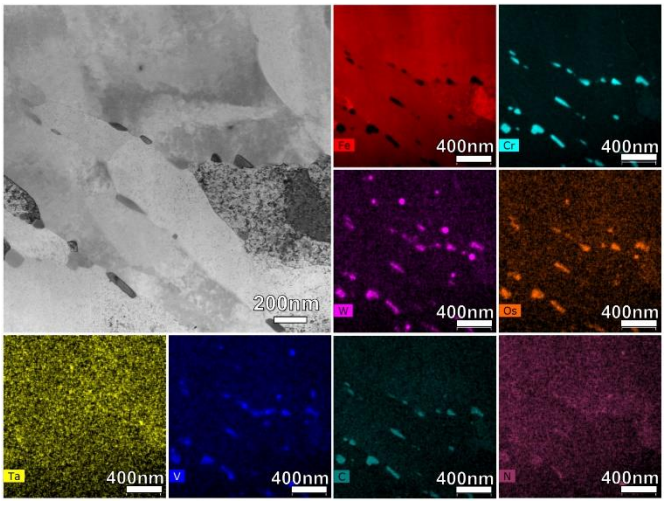

Fig. 2. Bright field (BF) TEM image of 72 dpa irradiated Eurofer97 and the corresponding STEM-EDS elemental mapping results of BF TEM image. 3×3 pixel smoothing applied.

High Dose Neutron Irradiation of Silicon Carbide Composites

Category: DOE-JAEA
Name: T. Koyanagi, Y. Katoh/T. Nozawa
Affiliation: ORNL/QST

For the development of silicon carbide (SiC) fiber reinforced SiC matrix (SiC/SiC) composites for fusion reactor structural applications, degradation of material properties due to intense neutron irradiation is a critical feasibility issue. The objective of this task is to obtain better understanding of the effects of high neutron fluence irradiation on the thermo-mechanical properties and microstructures.

This collaboration has achieved the milestone of neutron irradiation up to ~100 displacements per atom (dpa) with an equibalance of 1 dpa = 1×10^{25} n/m^2 (E >0.1 MeV). Neutron irradiation was conducted in the HFIR at ORNL. The total duration of the irradiation was 1000–1150 days. The material investigated was chemical vapor infiltrated SiC/SiC with Hi-Nicalon Type-S (HNS) fiber coated with a multi-layer pyrolytic carbon (PyC)/SiC interphase. Key physical and mechanical properties investigated included irradiation-induced swelling, thermal conductivity, proportional limit stress, and ultimate strength. For these properties, strength reductions predominantly determine the limitations of the materials at high neutron doses, whereas positive results have been reported for the other properties.

The length change of the specimens found that the SiC/SiC composites were dimensionally very stable at high neutron doses; swelling of SiC/SiC composites saturated at nominal neutron damage of ~1 dpa at elevated temperatures. This saturation behavior has been confirmed at up to 100 dpa at 300 and 600°C and up to 70 dpa at 800°C. Similar to swelling, changes in the thermal conductivity saturate at ~1 dpa. Although reduction of the thermal conductivity following irradiation is significant at low irradiation temperatures, the stable thermal conductivity at high doses is favorable for fusion applications.

Degradation of the mechanical properties at high neutron doses was irradiation-temperature dependent. The degradation of proportional limit stress and ultimate flexural strength was moderate at an irradiation temperature of 800°C. However, the proportional limit stress and ultimate flexural strength were significantly degraded due to irradiation at lower temperatures as show in Fig. 1. In case of the irradiation at 320°C, the quasi-ductile fracture behavior of the unirradiated composite became brittle after irradiation, which was explained by loss of functionality of the fiber/matrix interface associated with disappearance of interphase by irradiation (Fig. 2). The specimens irradiated at 630°C showed increased apparent failure strain because of the fiber/matrix interphase weakened by irradiation-induced partial debonding based on fractography. The fractography also suggested a loss of the fiber strength irradiated at 320°C.

In summary, this study provided critical experimental data on the effects of high-dose neutron irradiation on the composite properties. Improvement of the irradiation resistance has been pursued under this collaboration.

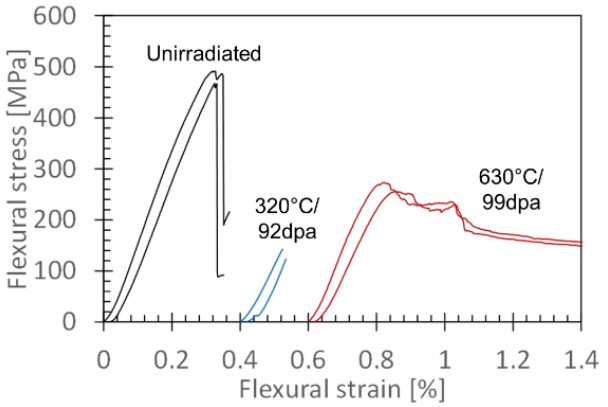

Fig. 1. Flexural behavior of unirradiated and irradiated SiC/SiC composites.

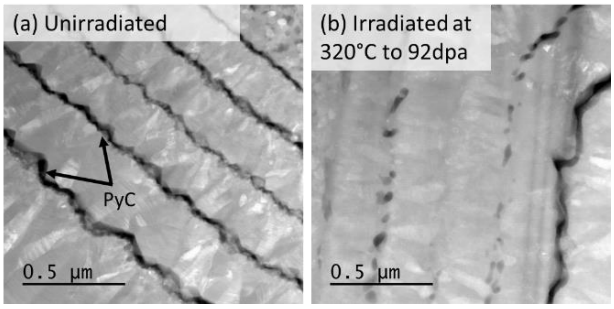

Fig. 2 STEM-HAADF micrographs of PyC/SiC multi-layer interphase: (a) unirradiated and (b) irradiated

HFIR Irradiation Campaigns in Support of the DOE/QST Fusion Materials Collaboration

Category: DOE/QST HFIR
Name: Y. Katoh, J.W. Geringer / H. Tanigawa, T. Nozawa
Affiliation: ORNL/QST

The Project Arrangement between JAERI, JAEA, now QST, MEXT of Japan and U.S. DOE, under the Cooperation in Research and Development in Energy and Related Fields, has been in effect for more than 37 years. The basis of this collaboration is the shared use of irradiation experiments in ORNL mixed spectrum fission reactors, first the ORR, then the HFIR reactor.

The objective of this collaboration is to design, conduct and evaluate joint irradiation experiments that partially simulate DT fusion irradiation conditions for the purpose of investigating the irradiation response of Japanese and U.S. structural and special purpose materials. The experiments target high levels of atomic displacement and helium content in order to establish the database on the properties and behavior of such materials and to evaluate their performance for the use in future fusion reactors.

During the last decade, HFIR has achieved 6 to 7 operating cycles per year, each lasting approximately 24 days at an operating power of 85 MW. It has remained operational and available for most of the period, except for the nearly year-long shutdown period that started in November 2018 and ended in October 2019, followed by another 6-month downtime period that started in August 2020 and ended February 2021, both due to issues related to fuel quality.

There have been a large number of collaboration irradiation campaigns, mostly exclusively for DOE/JAEA (now QST). The few exceptions include the RB-19J that was a three-party collaboration including the PHENIX Project. Table 1 lists the current ongoing campaigns supporting this collaboration, with 18 rabbit capsules now in reactor. Several ongoing PIE activities continue generating materials data and developing technology using the specimens from these campaigns.

The future plan for HFIR is to continue operation at least until 2035, when the potential renovations planned include replacing the reactor pressure vessel and converting to low enriched uranium (LEU). In the near-term future, HFIR plans replacement of the permanent beryllium reflector. Given the current schedule, this outage is planned for early 2024.

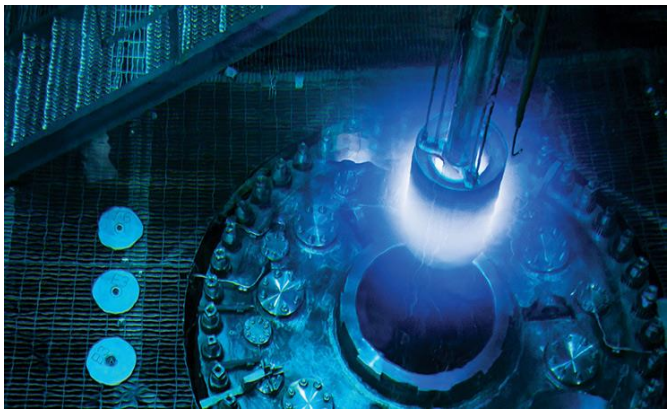

Fig. 1 HFIR top plate and fuel element shown during a refueling operation in 2015. (credit G. Martin/ORNL)

Table 1. Irradiation campaigns conducted in the HFIR reactor in support of the DOE-QST collaboration on fusion materials research and development.

Campaign	Years	Program	Facility	Material	Temperature (°C)	Max. Fluence ($x10^{25}$ n/m^2, E>0.1MeV)
JP-26/27	2004-2008	DOE/JAEA	Target	RAFMS	300/400	~20
JP-28/29	2005-2013	DOE/JAEA	Target	RAFMS	300/400/500	~80
RB-15J	2008-2009	DOE/JAEA	RB*	RAFMS	300/400	~6
JP-30/31	2011-2013	DOE/JAEA	Target	RAFMS	300/400/650	~20
RB-19J	2016	DOE/NIFS/JAEA	RB*	RAFMS, W	300-1200	~4
F8 Rabbits	2009-2013	DOE/JAEA	Target	RAFMS	300	~60
F11 Rabbits	2011-2013	DOE/JAEA	Target	RAFMS	300	~25
JCR11 Rabbits	2012-	DOE/JAEA	Target	SiC	950	10/30/50/100/200
J12 Rabbits	2013	DOE/JAEA	Target	RAFMS	300	1.5/6
F13 Rabbits	2014-2018	DOE/JAEA	Target	RAFMS	300	15/30
SCF Rabbits	2014-	DOE/JAEA	Target	SiC	600/950	10/30/100/200
FHC Rabbits	2018	DOE/QST	Target	RAFMS	300	~5
FMP Rabbits	2020	DOE/QST	Target	Cu	100 -350	5
FH Rabbits	2020-2021	DOE/QST	Target	RAFM	300	5